



Article

Hydrochemical and Isotopic Characterization of Groundwater in the Nakivale Sub-Catchment of the Transboundary Lake Victoria Basin, Uganda

Emmanuel Nabala Hyeroba ^{1,2,*} , Robert M. Kalin ^{1,*}  and Christine Mukwaya ²¹ Department of Civil and Environmental Engineering, University of Strathclyde, Glasgow G1 1XJ, UK² Directorate of Water Resources Management, Ministry of Water and Environment, Kampala 20026, Uganda; mukwayatina@yahoo.co.uk

* Correspondence: nabala.emmanuel91@gmail.com or nabala.emmanuel@mwe.go.ug (E.N.H.); robert.kalin@strath.ac.uk (R.M.K.); Tel.: +256-783553292 (E.N.H.); +44-7772025478 (R.M.K.)

Abstract: This study characterized groundwater resources for the Nakivale sub-catchment of the transboundary Victoria Basin in Uganda using classical hydrochemical and stable isotopic approaches. Groundwater in the study area is essential for domestic, agricultural, and industrial uses. As a sub-domain of the larger Victoria Basin, it also plays a crucial role in shaping the hydrological characteristics of this vital transboundary basin, both in terms of quality and quantity fronts. This makes its sustainable management and development vital. The predominant groundwater type is Ca-SO₄, with other types including Ca-HCO₃, Na-Cl, Na-HCO₃, and Ca-Mg-SO₄-Cl. Hydrochemical facies analysis highlights the importance of rock–water interactions in controlling groundwater chemistry, mainly through incongruent chemical weathering of Ca-rich plagioclase feldspars and the oxidation of sulfide minerals, such as pyrite, which are prevalent in the study area. Groundwater recharge is primarily influenced by the area’s topography, with recharge zones characterized by lineament networks, located in elevated areas. Stable isotope analyses indicate that groundwater mainly originates from local precipitation, while tritium data suggest the presence of both recent and older groundwater (likely over 20 years old). The study’s comprehensive approach and findings contribute significantly to the understanding of groundwater systems in the region, thus providing valuable insights for policymakers and stakeholders involved in water resource management and development strategies.

Keywords: hydrogeochemistry; isotope hydrology; precipitation; groundwater management; Victoria Basin; Nakivale; Isingiro; Uganda



Citation: Hyeroba, E.N.; Kalin, R.M.; Mukwaya, C. Hydrochemical and Isotopic Characterization of Groundwater in the Nakivale Sub-Catchment of the Transboundary Lake Victoria Basin, Uganda. *Water* **2024**, *16*, 3394. <https://doi.org/10.3390/w16233394>

Academic Editor: Lixin Yi

Received: 18 October 2024

Revised: 16 November 2024

Accepted: 20 November 2024

Published: 25 November 2024



Copyright: © 2024 by the authors. Licensee MDPI, Basel, Switzerland. This article is an open access article distributed under the terms and conditions of the Creative Commons Attribution (CC BY) license (<https://creativecommons.org/licenses/by/4.0/>).

1. Introduction

Water resources are integral to sustaining human life, fostering economic growth, and supporting biotic ecosystems, particularly in regions such as the Lake Victoria Basin, one of Africa’s most critical transboundary water systems [1]. The significance of these resources is underscored by global and regional frameworks, such as Sustainable Development Goal 6, Africa’s Agenda 2063 Goal 6, and Uganda’s National Development Plan 4, all of which advocate for easy and equitable access to safe and sustainable water resources [2–4]. Uganda’s Vision 2040, a long-term national development plan aimed at transforming the country into a modern and prosperous nation by 2040, projects significant growth in water demand as the country strives for a competitive upper middle-income status [5].

In the Nakivale sub-catchment in Southwestern Uganda, water demand is projected to rise substantially, with domestic, industrial, irrigation, and livestock needs expected to reach 6.3, 0.28, 0.81, and 0.46 MCM/year, respectively, by 2040 [6,7]. Without proper management, these resources may face depletion, threatening regional development and ecological balance [1,6–9]. The current water resource demand in the Nakivale sub-catchment ranges be-

tween 3.5–4.5 MCM/year [6], with groundwater recharge estimated at 50–100 mm/year [7]. This close range imbalance between water demand and recharge highlights the need for detailed studies on local hydrological processes, which are essential for the sustainable management of water resources in the region.

According to previous studies by [9,10], groundwater and surface water within the Lake Victoria Basin are closely interlinked. As a consequence, this symbiotic effect influences both the quantity and quality of water resources in the two hydrological systems. Despite this, critical aspects such as localized groundwater recharge processes, flow dynamics, and the factors influencing groundwater chemistry in the region remain poorly understood [1,7]. Therefore, this study aims to characterize groundwater within the Nakivale sub-catchment in Southwestern Uganda using both classical hydrochemistry and isotopic approaches.

These techniques have been globally used to infer information on groundwater origin, recharge processes, flow patterns, rock–water interaction processes among many more hydrological studies [10–18]. The specific objectives are to evaluate the key processes controlling groundwater hydrochemistry, determine the hydrogeochemical groundwater facies prevalent in the study area, analyze groundwater origin, recharge processes, and finally, formulate evidence-based policy recommendations for sustainable groundwater management and development within the Nakivale sub-catchment.

The findings of this study are not only relevant for the Nakivale sub-catchment but also have broader implications for the entire Lake Victoria Basin. As a transboundary water system shared by Uganda, Kenya, Tanzania, Rwanda, and Burundi, effective management of the Lake Victoria Basin's water resources requires a comprehensive understanding of the hydrological processes that govern water availability and quality at both localized and broader fronts. This enhances the understanding of groundwater dynamics in the study area and provides valuable insights for the wider management of the transboundary Lake Victoria Basin.

2. Materials and Methods

2.1. Study Area

The Nakivale sub-catchment is located in Isingiro district, southwestern Uganda (Figure 1). It serves as a tributary to the Rwizi Catchment which is also a tributary to the greater Victoria Basin [6]. The area spans over a total area of 760 square kilometers and is positioned within the country's water stressed area (locally referred to as a cattle corridor), where riparian communities travel long distances during drought spells in search for water from nearby deep boreholes and limited surface water bodies [1,6,7].

The study area predominantly consists of lowland surface remnants, occupying more than 60 percent of the sub-catchment. Infill areas are located in the western and eastern parts of the sub-catchment and are characterized by poorly sorted outwash fans. High-relief areas are positioned along the extreme margins of the catchment and are covered by upland surface remnants susceptible to erosion (Figure 1). The project area has a population estimate of over 616,700 people with most of the riparian communities staying within urban and peri urban centers [19]. It houses the fourth largest refugee camp in Uganda after Yumbe, Adjumani, and Arua districts. The area also registers an annual refugee influx estimate of 10,000–30,000 [20], and is a grazing spot for over 0.5 million cattle [6].

2.2. Climate

Nakivale lies within the equatorial zone of low pressure where winds typically remain light and variable [21]. Its weather patterns are notably influenced by the thermal equator, also known as the Inter-Tropical Convergence Zone (ITCZ), which acts as a zone of instability separating the converging air masses of the northern and southern hemispheres [1,6,7]. Characterized as hot and humid, the climate of the study area features two distinct rainy seasons (March to May and September to November), the later occasionally extending to December [6]. The dry seasons extend from December to February, and from June to

August. The wettest months typically occur in November and April, with July being the driest. Annual rainfall ranges from 966 mm to 1380 mm and is influenced significantly by factors such as topography, wetland systems, and open water bodies [1]. Average monthly temperatures range from a minimum of 27 °C to a maximum of 31 °C. The dew-point temperature averages around 19 °C, while the long-term average monthly temperature consistently surpasses 30 °C and occasionally peaks at 38 °C [6].

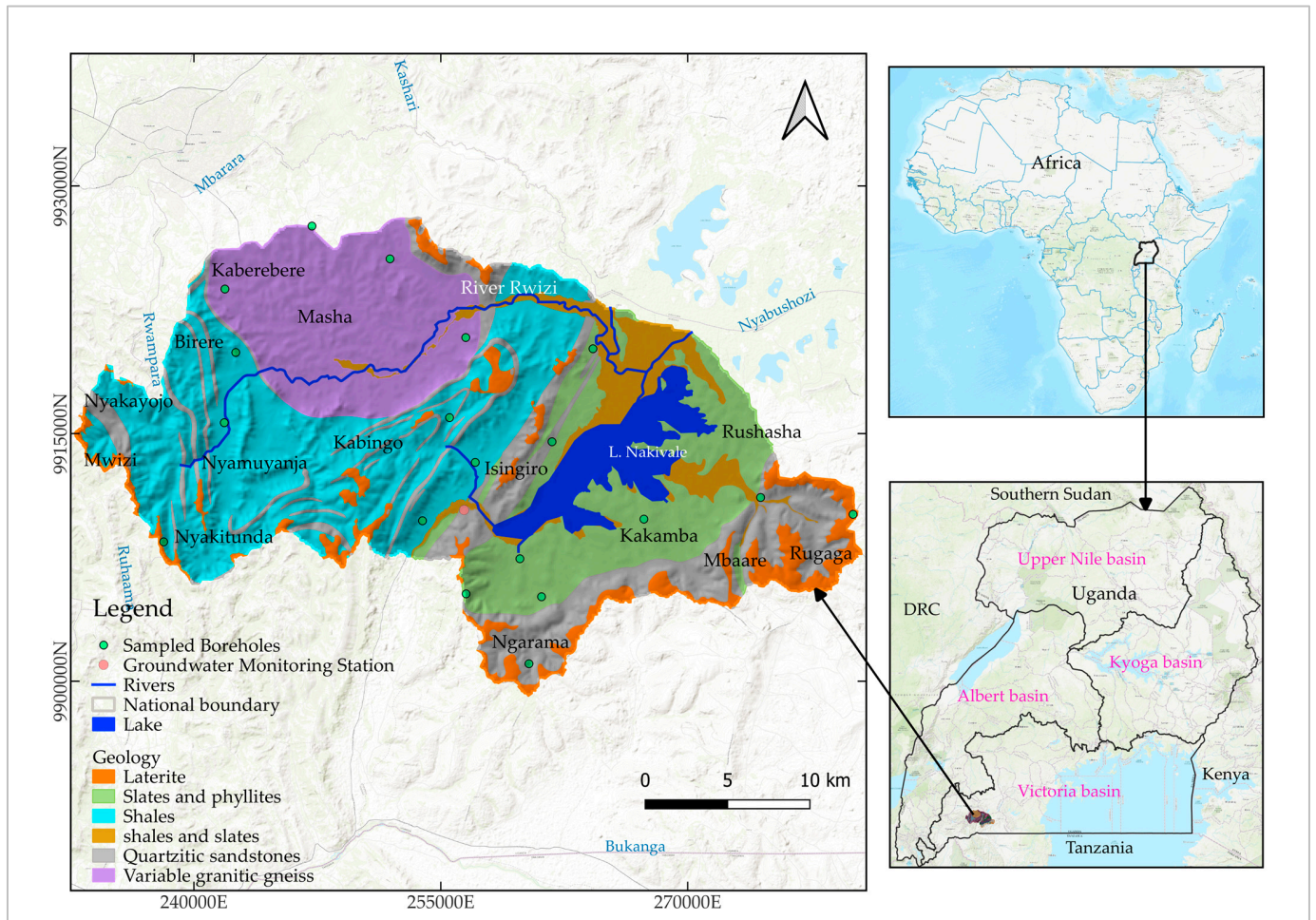


Figure 1. Location map of Nakivale sub-catchment within the Transboundary Victoria Basin, southwestern Uganda.

2.3. Geological Setting

The study area is overlain by the Proterozoic Karagwe-Ankolean system of rocks (1400–950 Ma) which is part of the Burundian belt in the eastern Democratic Republic of Congo [6,9]. This rock system rests unconformably on the Buganda-Toro rock system in Uganda which also overlies the Basement Complex rocks [22]. The Karagwe-Ankolean rock system consists of sedimentary to meta-sedimentary rocks that have been exposed to various grades of metamorphism, ranging from low to high [23].

The sedimentary facies within the Karagwe-Ankolean rock system comprise sandstones, shales, and conglomeratic lenses, while the metamorphic rocks include granite gneisses, phyllites, and schists. Sedimentary facies are common in elevated areas while the metamorphosed facies are present in lowlands, providing evidence of regional metamorphism and contact metamorphism near former areas of granitic intrusion [24]. These older rocks were intruded by younger variable granitic rocks that initially formed topographical highs but are now represented as low-lying areas due to the susceptibility of granites to

weathering. The current topography can be attributed to differential weathering between the older host rocks and the younger granitic rocks [25].

The dominant minerals in this area are silicate minerals, ranging from felsic silicates (quartz, muscovite and orthoclase) to mafic silicate minerals (plagioclase feldspars and minerals of the Bowen discontinuous series) [16]. This is due to varying episodes of variable granitic intrusions (G1-G4) that the region experienced [26]. Muscovite schists and phyllites intercalated with quartzites are also common within the lower Karagwe-Ankolean rock system where the project area lies [9,26]. Occasional calc-silicate rocks are also common in the study area [25]. According to [22], the Karagwe-Ankolean rock system is also characterized by sulfide rich minerals such as chalcopyrite, pyrite, galena, and sphalerite evident in Kitaka (Mbarara district) and Gayaza (Isingiro district).

2.4. Hydrogeology

The hydrogeology of the Nakivale sub-catchment is primarily shaped by the region's underlying geology. The area is predominantly composed of argillaceous, impermeable rock types such as shales, slates, phyllites, and granite gneisses (Figure 1). These low-permeability lithologies result in high surface runoff, limiting groundwater recharge. Groundwater infiltration occurs mainly through fractured networks and bedding planes, where structural weaknesses allow for some permeability [27–29].

Groundwater flow in the study area is largely controlled by the hydraulic head gradient which closely follows the natural topography (Figure 2). The flow pattern is predominantly local, with groundwater moving through shallow aquifers over short distances. In certain areas, particularly in the western and eastern parts of the sub-catchment, intermediate groundwater flow systems exist, indicating slightly longer flow paths. Previous studies by [30–32] identified three main aquifer types in the region: weathered/fractured aquifers, fluvial aquifers, and paleochannels. The weathered and fractured aquifer system typically occurs at depths greater than 60 m [31], though this can vary. Permeability is highest near the fracture-saprolite interface and is determined by the number, distribution, and connectivity of fractures [30,31].

Fluvial aquifers consist of consolidated and unconsolidated sediments and are generally shallow [6]. Their hydraulic properties depend on sediment sorting, size, and packing, with well-sorted sediments exhibiting higher permeability [33]. These aquifers can be unconfined or semi-confined, with fine riverbed material often creating confined conditions [30]. According to [31], paleochannel aquifers formed by historic river reversals also serve as significant aquifers in the region. These ancient river channels are filled with thick sediment deposits, including gravels and sands, and provide high groundwater yields, often exceeding 50 cubic meters per hour [34]. In areas like Rukungiri in southwestern Uganda, paleochannels are known for their high aquifer productivity due to the thick alluvial deposits [31].

Over the past three years, groundwater levels at the Isingiro groundwater monitoring station in the study area have notably fluctuated (Figure 3). From January 2021 to mid-2023, these levels exhibited a declining trend, indicating over-extraction or inadequate recharge during that time. Groundwater levels at this station respond to rainfall with a time lag of 1–2 months, reflecting low recharge rates in the area (Figure 3). The recent increase in groundwater recharge can be partly attributed to catchment restoration activities in the Rwizi catchment since 2021, as well as two significant flooding events: one in May 2023 and the El Nino flood event in November 2023 [35,36]. Additionally, potential changes in confining pressure related to land use and aquifer recharge processes can play a role in controlling piezometric surfaces [37]. Therefore, it is evident that effective groundwater management is essential for the sustainable use of groundwater resources in the study area.

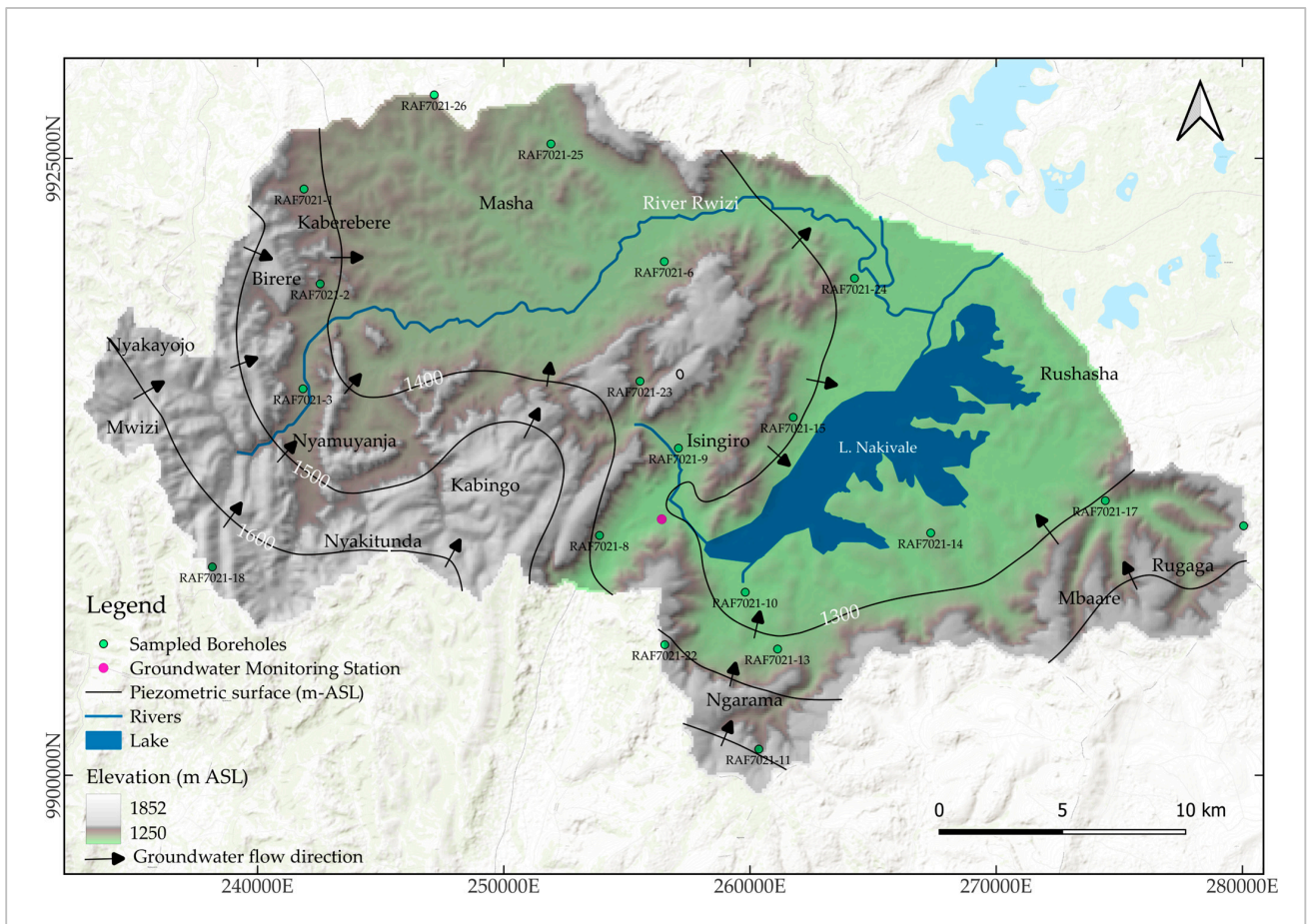


Figure 2. Groundwater flow patterns within the Nakivale sub-catchment, southwestern Uganda.

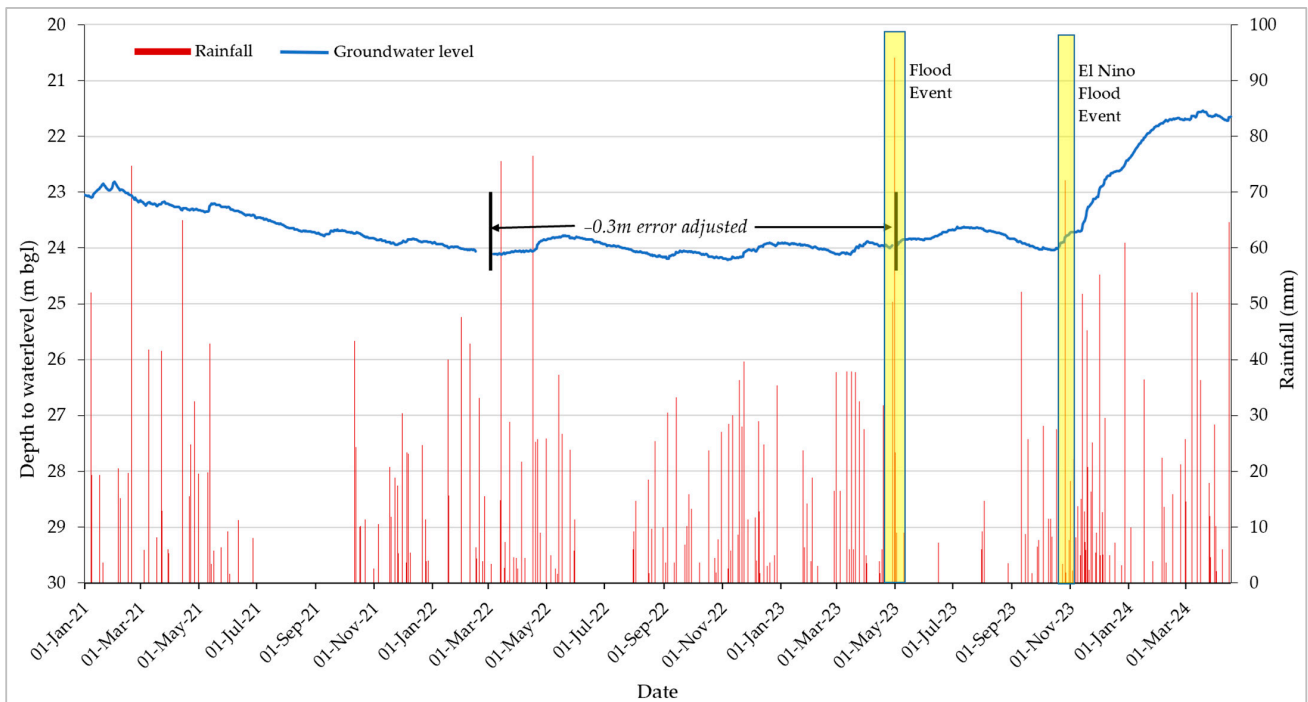


Figure 3. Hydrograph showing groundwater trends at Isingiro groundwater monitoring station between 2021 and 2024 (data source: Ministry of Water and Environment, 2024).

2.5. Sample Collection and Analysis

Sampling points were strategically selected to account for hydrogeological variations in the study area. Groundwater samples were collected from 19 boreholes in the study area (Figure 1). Sampling occurred from 15 February 2024 to 20 February 2024 during the dry season. Field measurements of pH, redox potential (Eh), dissolved oxygen (mg/L), temperature (°C), and electrical conductivity ($\mu\text{S}/\text{cm}$) were obtained in situ using a calibrated HANNATM multi-parameter meter (HI 9829_S/N 07100011101). Total alkalinity was analyzed in situ by acid–base titration using 0.02 M hydrochloric acid. Water samples for cations and anions were collected in 500 mL HDPE bottles and tightly capped to prevent any leakage. Samples intended for cation analysis underwent filtration using GF/C filter papers and were then acidified with concentrated nitric acid of analytical grade to achieve a pH of less than 2. For tritium and stable isotope analysis (Deuterium and oxygen-18), water samples were respectively collected in 500 mL HDPE bottles and 50 mL HDPE bottles.

The major ions, namely, Na^+ , K^+ , Ca^{2+} , Mg^{2+} , Cl^- , NO_3^- , and SO_4^{2-} , were analyzed in mg/L using the ion chromatography method. Al, Fe, Si, and B were analyzed in their elemental forms using the Inductively Coupled Plasma Mass Spectrometry (ICP-MS) method. This method allows for the highly sensitive and precise measurement of elements at very low concentrations [38]. The stable isotopes, ^2H and ^{18}O in each water sample were estimated using laser absorption spectroscopy. The results possess an accuracy of $\pm 0.2\%$ for $\delta^{18}\text{O}$ and $\pm 1.6\%$ for $\delta^2\text{H}$. Tritium concentration was determined with an accuracy of ± 0.2 TU using liquid scintillation counting (LSC), a method known for its high sensitivity and accuracy [39].

2.6. Hydrochemical Data Analysis

2.6.1. Groundwater Facies Analysis

This analysis involved graphical representation of the cationic (Ca^{2+} , Mg^{2+} , $\text{Na}^+ + \text{K}^+$) and anionic (HCO_3^- , SO_4^{2-} , Cl^-) chemical species on a Piper diagram using Origin Pro Version 2022, a statistical software. The respective concentrations (meq/L) were normalized to 100% and then plotted as points on a Piper diagram. The position of each plot on a piper diagram serves as an estimate for the groundwater type inherent to the sampled well [40].

2.6.2. Groundwater Hydrochemical Evolution Assessment

(i) The Gibbs plot

The Gibbs plot involved plotting total dissolved solids (TDS) against the quotient factor of major cations for the cationic Gibbs plot (Equation (1)) and TDS against the quotient factor of major anions for the anionic Gibbs plot (Equation (2)). According to [41], this model offers insights into three key mechanisms that influence groundwater chemistry: atmospheric precipitation dominance, rock weathering dominance, and evaporation-crystallization dominance.

$$\text{Gibbs Cationic Ratio} = \frac{\text{Na}^+ + \text{K}^+}{\text{K}^+ + \text{Na}^+ + \text{Ca}^{2+}} \quad (1)$$

$$\text{Gibbs Anionic Ratio} = \frac{\text{Cl}^-}{\text{Cl}^- + \text{HCO}_3^-} \quad (2)$$

(ii) Multivariate analysis

This utilized both the R-mode and Q-mode hierarchical cluster analysis (HCA), along with the Factor Analysis approach, using Origin Pro version 2022. R-mode and Q-mode HCA group variables and samples, respectively, to identify relationships and possible common sources or processes affecting these parameters [18,42–44]. These clusters can reveal spatial or temporal patterns in groundwater quality and can be instrumental in identifying distinct facies or regions influenced by similar geochemical processes [13]. Factor Analysis was used to complement HCA by reducing the dimensionality of hydrochemical data and identifying the most significant factors influencing groundwater chemistry [44].

2.6.3. Geochemical Modelling

This approach utilized the Geochemist's Workbench Community Edition 17.0 software to calculate the saturation indices (SI) of different mineral species as well as the partial pressure of carbon dioxide for each groundwater sample. The saturation index was estimated as the logarithm of the ratio of the ion activation product (IAP) to the solubility product (K_{sp}) of dissolving species.

$$SI_{\text{Calcite}} = \log \frac{IAP}{K_{sp}} \quad (3)$$

The calcite saturation index and partial pressure of carbon dioxide provide insights into the potential sources of bicarbonates within groundwater [45,46]. They also shed light on the incongruent weathering of silicates or other forms of chemical weathering [45].

2.6.4. Spatial Analysis Using GIS Tools

Spatial analysis utilized Quantum Geographical Information System (QGIS) Version 3.36.3. The spatial analytical tools employed in this study include, but are not limited to, interpolation and raster analysis tools. The interpolation tool used in this study was the ordinary kriging interpolation tool which is ideal for datasets with unknown trends such as hydrochemical datasets [47]. This tool assumes a constant mean and variance across the interpolated field [48]. It is particularly suitable for hydrochemical assessments [13,47,48].

2.7. Isotope Analysis

2.7.1. Stable Isotope Analysis

This involved characterizing the isotopic signature of rainfall in the area through establishment of a local Deuterium excess (D-parameter) line for the Nakivale sub-catchment. This approach has been widely adopted for tracing the origin of groundwater [12,17,49]. Deuterium excess values in precipitation were calculated to identify the moisture source for rainfall received within the study area (Equation (4)).

$$\text{Deuterium excess} = \delta^2H - 8\delta^{18}O \quad (4)$$

where δ^2H and $\delta^{18}O$ are deuterium and oxygen-18 values in local precipitation, respectively.

The obtained D-excess values were used to generate the D-parameter line for the Nakivale sub-catchment using Equation (5).

$$\delta^2H = 8 * \delta^{18}O \pm \text{Mean}(D - \text{excess value}) \quad (5)$$

The D-parameter line was then plotted alongside the Global Meteoric Waterline (GMWL) on the δ^2H vs. $\delta^{18}O$ graph. The GMWL is represented by Equation 6 [50]. The shift of the D-parameter line from the GMWL provided insights into the moisture sources for precipitation received within the study area [51,52].

$$\delta^2H = 8 * \delta^{18}O + 18 \quad (6)$$

2.7.2. Tritium Isotope Analysis

According to [53], interpreting tritium values involves comparing tritium concentrations with known atmospheric input levels from local precipitation. This comparison helps reconstruct groundwater recharge histories and assess the sustainability of aquifer resources in the study area [53,54]. However, it is important to note that there are no historical tritium measurements for precipitation received within the project area and nearby isotope stations. Therefore, this study adopted a proxy approximation: tritium unit values less than 0.4 to indicate groundwater likely to be older than 20 years and tritium unit values greater than 0.4 to indicate recent groundwater water recharged less than 20 years ago.

2.8. Groundwater Recharge Assessment

The assessment of groundwater recharge employed a multifaceted approach, integrating hydrogeochemical evolution analysis with the examination of the local groundwater flow network through geospatial analysis of hydraulic head gradients. The hydrogeochemical analysis focused on evaluating the groundwater's chemical properties as they evolve along its flow path, providing insights into the transformation of these properties along hypothetical recharge-discharge gradients. Additionally, analyzing the piezometric surface in relation to the area's geomorphology and structural geology offered a deeper understanding of active groundwater recharge zones.

3. Results and Discussion

3.1. Chemical Analysis

The chemical parameters show a range of variability across the samples. pH values range from 4.5 to 9.3 with a mean of 6.7 and a low standard deviation (SD) of 1.0, indicating consistency. Bicarbonate (HCO_3^-) has a wide range (10.0–439.3 mg/L) and a high SD (134.0), reflecting significant variability. Chloride (Cl^-) and nitrate (NO_3^-) show moderate variability, while sulphate (SO_4^{2-}), calcium (Ca^{2+}), and alkalinity exhibit considerable fluctuation. Sodium (Na^+), potassium (K^+), and magnesium (Mg^{2+}) have moderate variability. Total iron (Fe) ranges from 0.02 to 5.1 mg/L with a high SD of 1.5, indicating large fluctuations, with some samples showing minimal iron and others being significantly higher. Electrical conductivity (EC) also shows significant variation (297.0–1538.0 $\mu\text{S}/\text{cm}$) with a high SD of 366.3 (see Table 1).

Table 1. Descriptive statistics of major analyzed chemical parameters for 19 groundwater samples.

Chemical Parameter	Mean	Standard Deviation (SD)	Maximum	Minimum
pH	6.7	1.0	9.3	4.5
HCO_3^- (mg/L)	141.5	134.0	439.3	10.0
Cl^- (mg/L)	48.6	25.6	96.1	16.0
NO_3^- (mg/L)	16.4	14.1	46.1	0.0
SO_4^{2-} (mg/L)	204.7	148.9	515.6	29.9
Na^+ (mg/L)	59.9	27.4	134.6	8.7
K^+ (mg/L)	6.6	3.8	15.1	2.8
Mg^{2+} (mg/L)	23.5	15.6	51.5	0.0
Ca^{2+} (mg/L)	59.0	42.3	144.0	0.7
Total Fe (mg/L)	0.8	1.5	5.1	0.02
Alkalinity (mg/L CaCO_3)	145.2	136.1	445.3	11.4
EC ($\mu\text{S}/\text{cm}$)	746.8	366.3	1538.0	297.0

3.2. Mechanisms Controlling Groundwater Hydrochemistry

All groundwater samples fall within the rock-weathering dominance region of the Gibbs diagram. This clearly indicates that rock weathering is the predominant geochemical process shaping groundwater chemistry in the study area. These findings align with those of [16], who also attributed rock weathering processes as the primary mechanism controlling groundwater hydrochemistry in the region.

The relative position of each groundwater sample on the Gibbs diagram is primarily influenced by the Gibbs ionic ratio in relation to total dissolved solids [55]. When anionic plots tend toward a ratio of 1, it suggests Cl^- dominance. Similarly, when cationic plots approach a ratio of 1, it suggests $\text{Na}^+ + \text{K}^+$ dominance. From the Gibbs plots, it is evident that the exchanging cations are less of $\text{Na}^+ + \text{K}^+$ relative to Ca^{2+} for the ionic species and less of Cl^- relative to HCO_3^- for the anionic species. However, these interpretations should be treated with caution, as other principal hydrochemical components of groundwater, such as SO_4^{2-} and Mg^{2+} , are not considered in the Gibbs graphical model (Figure 4).

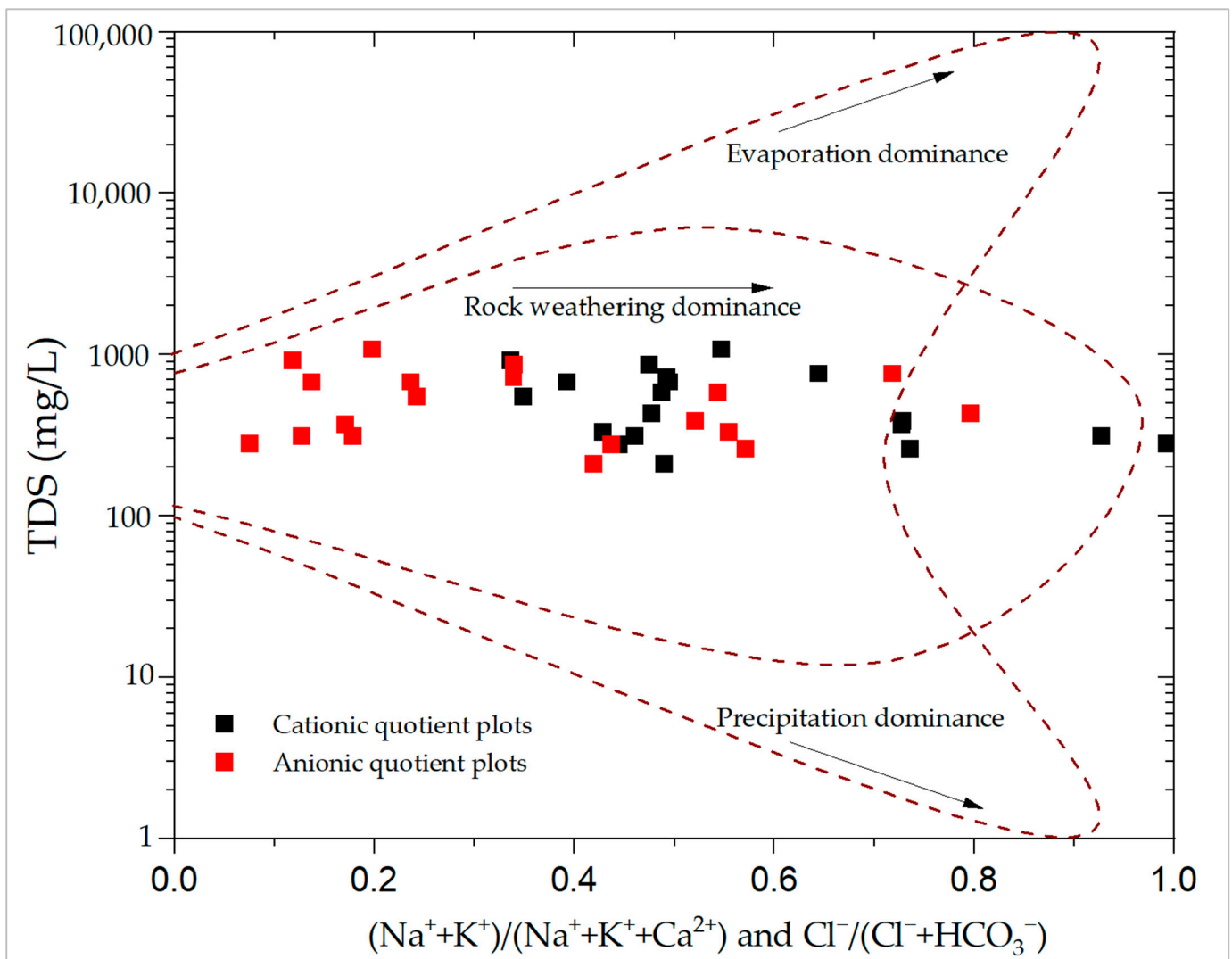


Figure 4. Cationic and anionic Gibbs plot for analyzed groundwater samples.

There is evidence of the Chebotarev sequence of groundwater hydrochemical species along groundwater flowlines within the study area (Figure 5). This sequence indicates that groundwater hydrochemistry evolves in the following order as it moves along a pathway: $\text{HCO}_3^- \rightarrow \text{HCO}_3^- + \text{SO}_4^{2-} \rightarrow \text{HCO}_3^- + \text{SO}_4^{2-} + \text{Cl}^- \rightarrow \text{SO}_4^{2-} + \text{Cl}^- \rightarrow \text{Cl}^-$ [56]. Therefore, water dominated by HCO_3^- suggests young, shallow groundwater or a localized flow pattern, while water dominated by Cl^- provides evidence of older groundwater or a regional flow pattern [16].

3.3. Groundwater Facies Analysis

The identified cationic groundwater types in the area include Ca, Mg, and Na, while the anionic groundwater facies consist of SO_4 , HCO_3 , and Cl. Based on the diamond-shaped Piper plot, these groundwater facies in the study area are further classified into Ca-Mg- SO_4 -Cl and a mixed water type comprising Na- HCO_3 and Ca-Mg- SO_4 -Cl (Figure S2). To address the bias posed by summing up hydrochemical facies within the Piper plot, the analysis of dominant hydrochemical species was further refined using 1:1 trendline plots. This approach helped to accurately characterize the dominant hydrochemical species and identify potential geogenic sources of ions and weathering processes.

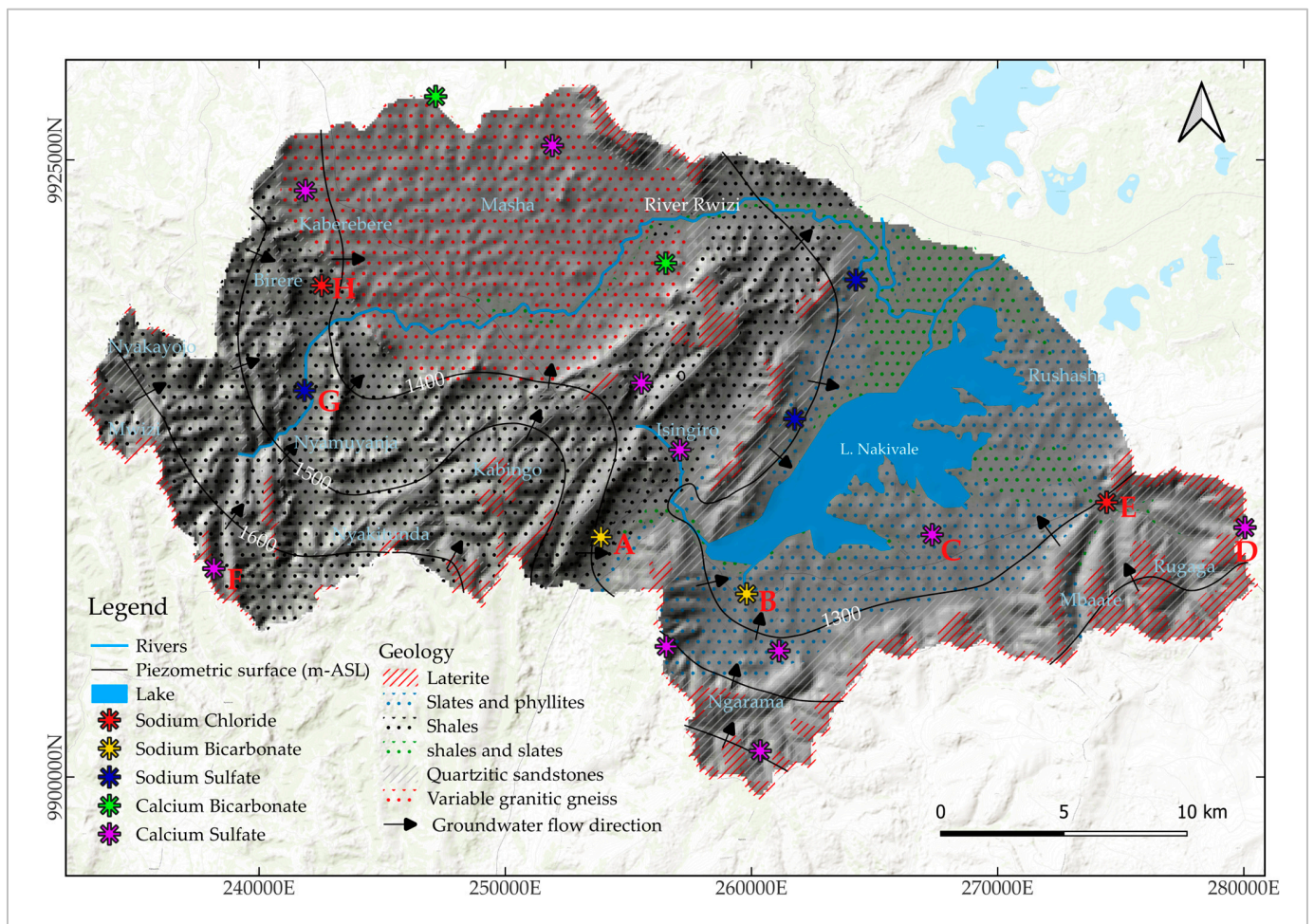


Figure 5. Evidence of groundwater evolution along groundwater flow path lines. The hydrochemical evolution of groundwater from within the study area can be traced from points D-E, F-G-H, and from A-B-C.

Figure 6a reveals that Ca^{2+} is more dominant as compared to Mg^{2+} . Therefore, the cationic facies in the Nakivale sub-catchment groundwater are ordered by relative abundance as $\text{Ca} > \text{Na} > \text{Mg} > \text{K}$. The 1:2 trendline represents potential incongruent weathering of Ca-rich plagioclase feldspars (Equation (9)). Figure 6c clearly shows that the dominant anionic species is SO_4 evidenced by 90% of groundwater samples plotting above the SO_4^{2-} vs. Cl^- 1:1 trendline. Therefore, the anionic species are ordered by relative abundance as $\text{SO}_4 > \text{HCO}_3 > \text{Cl}$. These findings also align with the results of [16], which suggested the prevalence of Ca- SO_4 rich waters within southwestern Uganda.

Figure 6b reveals that the occurrence of Na-Cl groundwater facies is minimally due to halite dissolution, as only 16% of the points plot along the halite dissolution line. This is further evidenced by a weak correlation coefficient of less than 0.5 between Na^+ and Cl^- (Table S3). Most plots fall toward the sodium side, thus indicating another potential source of Na ions, possibly the weathering of Na-rich plagioclase feldspars. The 2:1 trendline indicates a potential cation exchange of Ca^{2+} for Na^+ in groundwater.

Figure 6d reveals that gypsum dissolution is less predominant within the study area. This is evidenced by only a few groundwater samples (26%) plotting along the gypsum dissolution line. This trend indicates that Ca and SO_4 ions are derived from other sources other than gypsum dissolution. The 1:2 trendline signifies potential ion exchange of Ca^{2+} for Na^+ in groundwater.

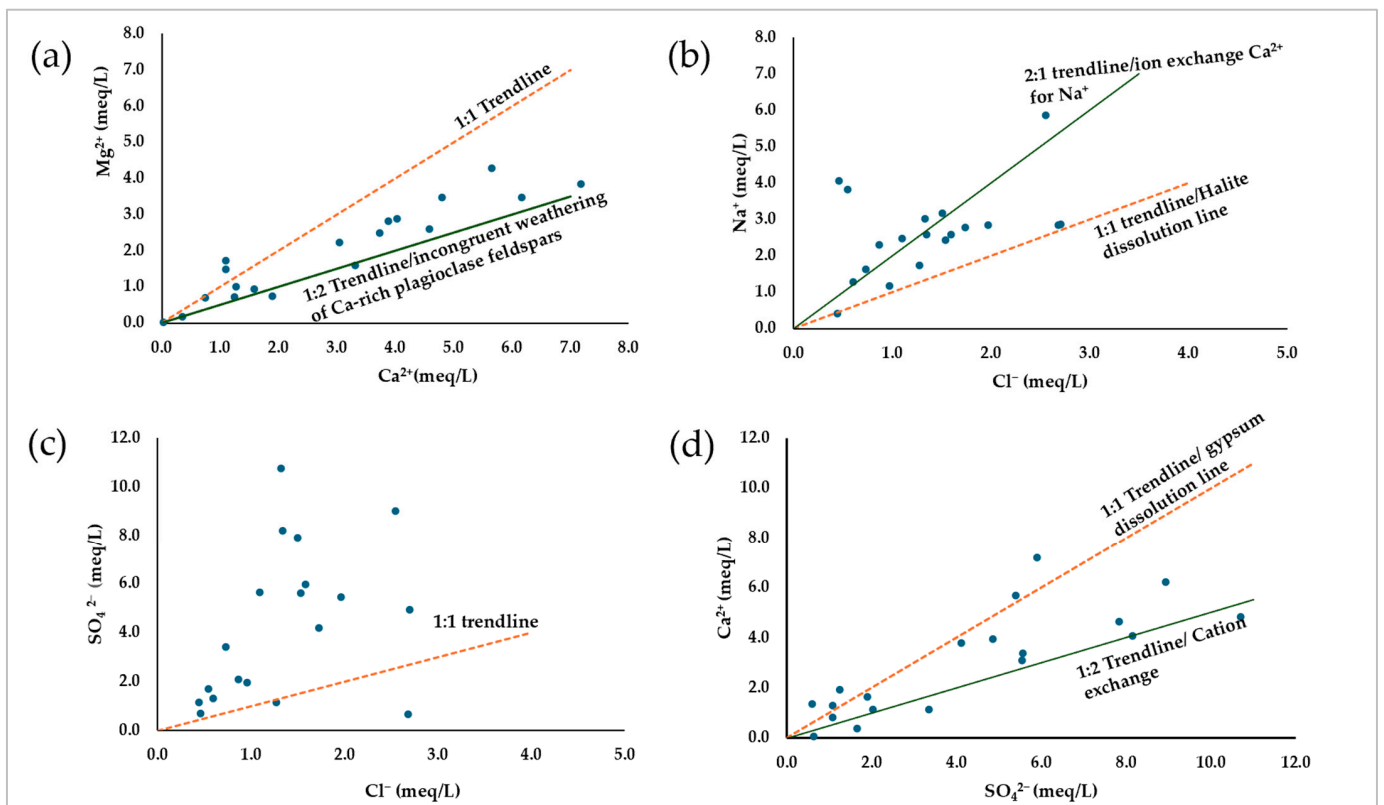
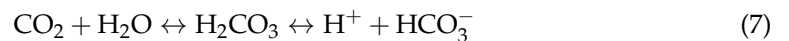
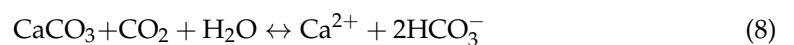


Figure 6. Bivariate plots showing dominant chemical species and potential weathering processes.

Figure 7 indicates that HCO_3^{-} in groundwater is not primarily due to calcite dissolution. Instead, it likely results from the dissolution of soil CO_2 derived from organic matter decay and microbial respiration as groundwater infiltrates (Equation (7)).

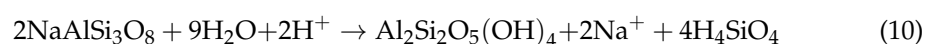


Typical atmospheric pCO_2 is around $10^{-3.5}$ atm [57]. In total, 95% of the sample values indicate higher dissolved CO_2 concentrations typical of groundwater influenced by soil CO_2 or microbial respiration and 16% of the samples exhibit positive SI_{calcite} values indicating that these samples are oversaturated with calcite mineral [46].



High pCO_2 and negative SI_{calcite} values also suggest active groundwater recharge with recent infiltration of CO_2 -rich water, whereas lower pCO_2 and increasing SI_{calcite} values may indicate the progression of groundwater away from recharge areas to discharge areas with potential for calcite precipitation as CO_2 degasses [57].

There exists a negative correlation between the partial pressure of carbon dioxide (pCO_2) and pH in groundwater (Figure S3). This can be attributed to the consumption of hydrogen ions (H^{+}) during silicate incongruent weathering [58]. H^{+} ions are consumed as they react with silicate minerals to produce clay minerals (such as kaolinite) and dissolved ions (like bicarbonate and silica) [59]. This consumption of H^{+} ions reduces the acidity of the water leading to an increase in pH.



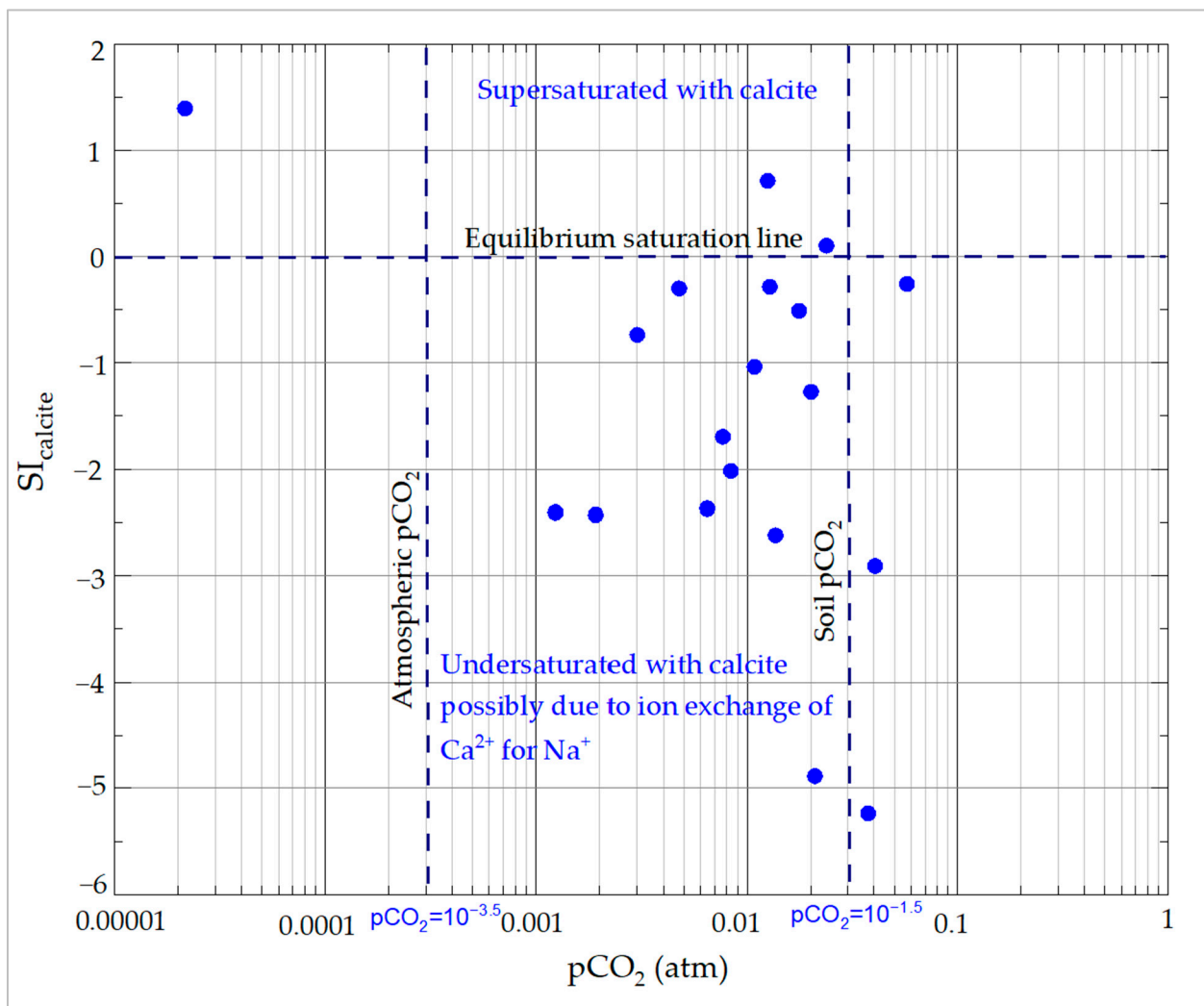
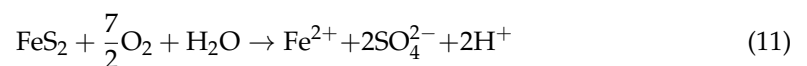


Figure 7. Calcite saturation index (SI_{calcite}) vs. partial pressure of CO_2 ($p\text{CO}_2$).

The redox potential (Eh) vs. pH, Pourbaix plot for a pyrite–water system, indicates that 90% of the samples fall within the pyrite region (Figure 8). Therefore, the dominance of sulphate anionic facies within groundwater in the study area primarily results from the oxidation of pyrite [60].



3.4. Hierarchical Cluster Analysis

The R-mode cluster analysis of variables identified three clusters of hydrochemical facies (Figure 9a). Cluster 1 includes the ionic species K^+ , Na^+ , Fe^{2+} , Cl^- , HCO_3^- , and Br^- . Cluster 2 comprises SO_4^{2-} , Mg^{2+} , and Ca^{2+} , while Cluster 3 consists of NO_3^- , Al^{3+} , and Si. pH is more closely correlated with the ionic species in Cluster 1, and electrical conductivity (EC) is more correlated with the ionic species in Cluster 2. The presence of these ions is likely due to a combination of natural geological processes and human activities. The detection of chloride and bromide points to potential anthropogenic sources such as agricultural runoff or industrial activities [62].

Cluster 2 contains bivalent ions typically associated with natural mineral weathering. Sulphates potentially originate from the weathering of rocks rich in sulfides such as FeS_2 which is common in the area [22]. The correlation of pH with these ions indicates that their concentrations in solution are mainly influenced by pH, particularly during the hydrolysis

of plagioclase minerals. The presence of sulphate further underscores the influence of both natural geological processes and potential anthropogenic sources such as the use of agricultural fertilizers [60].

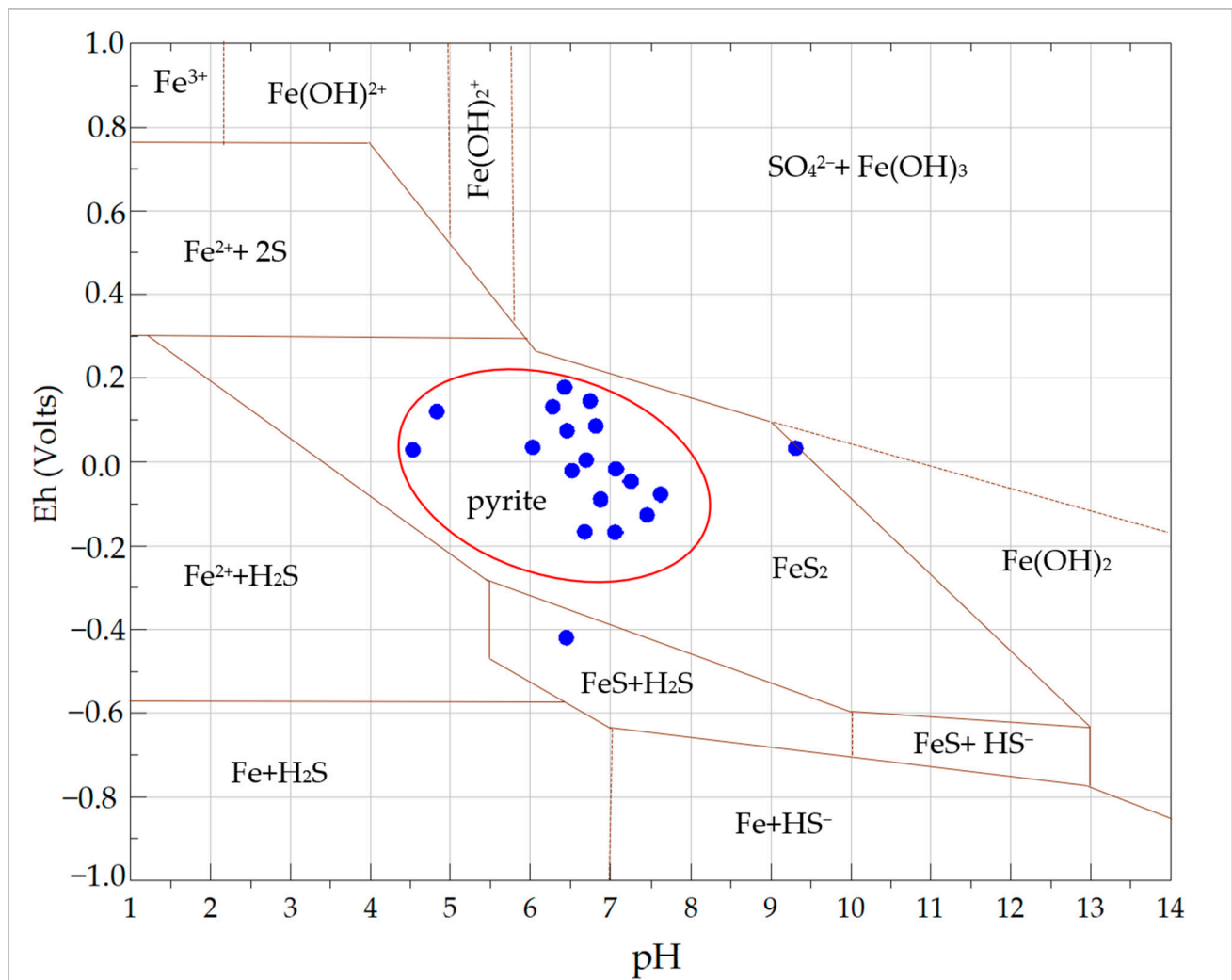


Figure 8. Pourbaix diagram for Fe-S-H₂O system at 25 °C 10⁻⁵ M dissolved species [61].

Cluster 3 ions reflect both natural and anthropogenic influences. Nitrate often indicates agricultural activity such as the use of nitrogen-based fertilizers or contamination from septic systems [63,64]. Aluminium and silicon are typically derived from the weathering of silicate minerals [65]. This cluster shows a blend of natural mineral weathering and human-induced contamination.

The Q-mode cluster analysis grouped groundwater samples into three groups based on their similarity in hydrochemical signatures. Group 1 includes samples RAF7021-1, RAF7021-9, RAF7021-11, RAF7021-13, RAF7021-14, RAF7021-23, and RAF7021-25. Group 2 consists of samples RAF7021-2, RAF7021-8, RAF7021-10, RAF7021-15, RAF7021-17, RAF7021-18, RAF7021-21, RAF7021-22, RAF7021-24, and RAF7021-26. Lastly, Group 3 comprises samples RAF7021-3 and RAF7021-6 (Figure 9b).

Group 1 groundwater samples exhibit moderate electrical conductivity (EC), indicating moderate mineral presence. The pH levels range from slightly acidic to slightly basic with an average around neutral (7.1). This group also has moderate levels of chloride (Cl⁻) and nitrate (NO₃⁻) with variability in HCO₃⁻ and SO₄²⁻ concentrations, indicating diverse sources of mineralization [18]. The water types in this group include Ca-Mg-SO₄-HCO₄, Ca-Mg-SO₄, and Ca-Mg-SO₄-HCO₃.

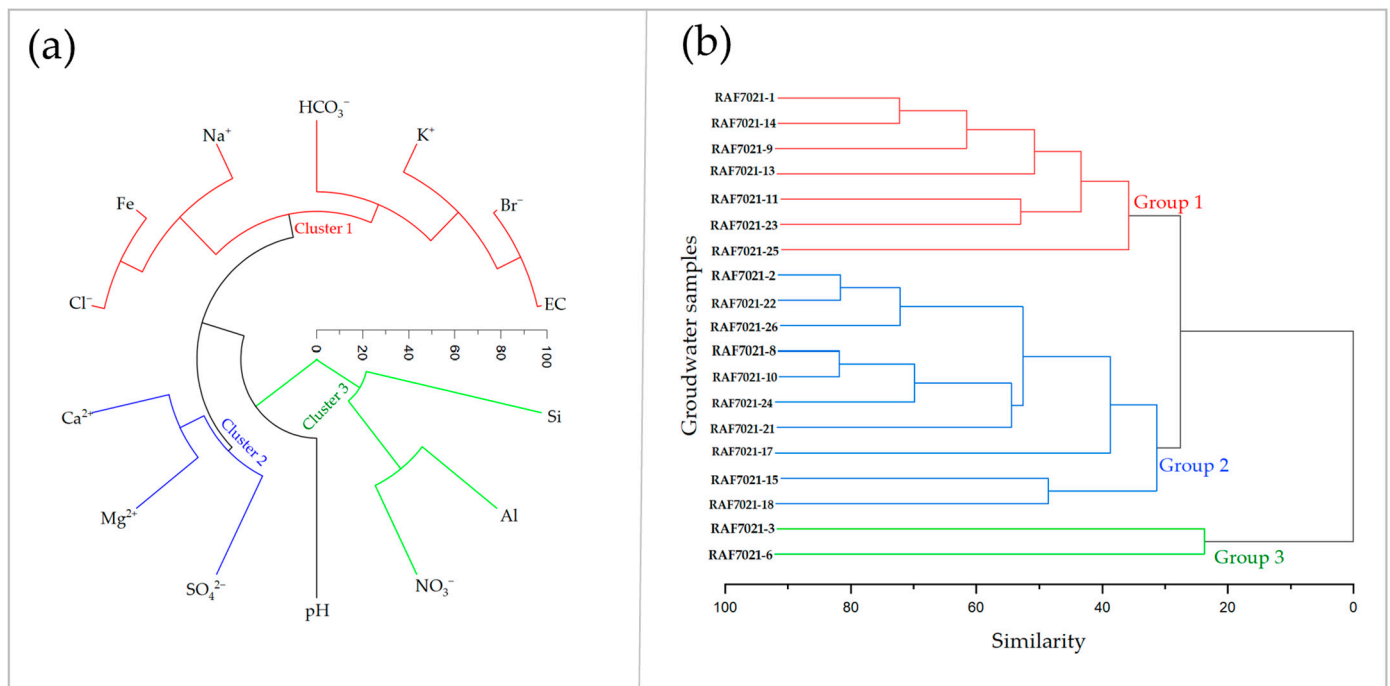


Figure 9. Dendrogram showing (a) chemical variables; (b) groundwater samples, clusters based on their chemical similarity.

Group 2 groundwater samples have lower electrical conductivity compared to Group 1, reflecting lower mineral content. The pH values are more variable, with some samples being notably more acidic. The concentrations of HCO₃⁻, Cl⁻, and SO₄²⁻ are generally lower than in Group 1. However, this group shows high variability in nitrate NO₃⁻ levels indicating potential diverse contamination sources [63,64]. This group's lower mineral content and variable pH suggest different hydrochemical processes [66]. The water types in this group are varied including Na-Cl-SO₄, Na-HCO₃, Ca-Mg-SO₄, and Ca-Mg-SO₄-HCO₃.

Group 3 groundwater samples show the highest electrical conductivity and bicarbonate HCO₃⁻ levels, indicating very high mineral content. The pH values in this group are relatively stable, averaging around 7.3 (slightly basic). This group also has significantly higher concentrations of SO₄²⁻ and Ca²⁺. The dominant water type in Group 3 is Ca-SO₄.

3.5. Analysis of Stable Isotope in Local Precipitation

Stable isotope data from 11 isotope stations near the study area, within Uganda and Rwanda obtained from the IAEA GNIP website, reveal variations in stable isotope signature across the region (Table S1). Mean δ²H values range from -7.099 to 10.845, while mean δ¹⁸O values range from -3.497 to -0.272. There is an altitude effect on the isotopic composition of rainfall in the study area (Figure 10). This is attributed to the temperature gradients associated with elevation differences [51]. Low-altitude areas are associated with high temperatures that enhance heavy isotope enrichment, whereas high-altitude areas experience lower temperatures that result in heavy isotope depletion [67].

The majority (90%) of stations show a mean Deuterium (D) excess value higher than the global average of 10 computed by [50]. The high D-excess values (>10) observed in local precipitation, along with findings from studies by [10,68,69], suggest local atmospheric moisture recycling processes within the region. This localized effect can be attributed to the influence of the Great Lakes (particularly Lake Victoria) on local precipitation.

D-excess histograms indicate that both the SON (September–October–November) and MAM (March–April–May) rainy seasons exhibit moderate variability, with the highest frequencies in the mid-range bins (Figures S4 and S5). The SON season's D-excess values suggest more uniform and stable moisture sources with limited atmospheric mixing. In

contrast, the MAM season shows a slightly broader range. However, the consistency in moisture sources across seasons, despite some variability, underscores the dynamic atmospheric processes in the study area and can be attributed to the effects of the Intertropical Convergence Zone (ITCZ) shift on rainfall patterns in the region.

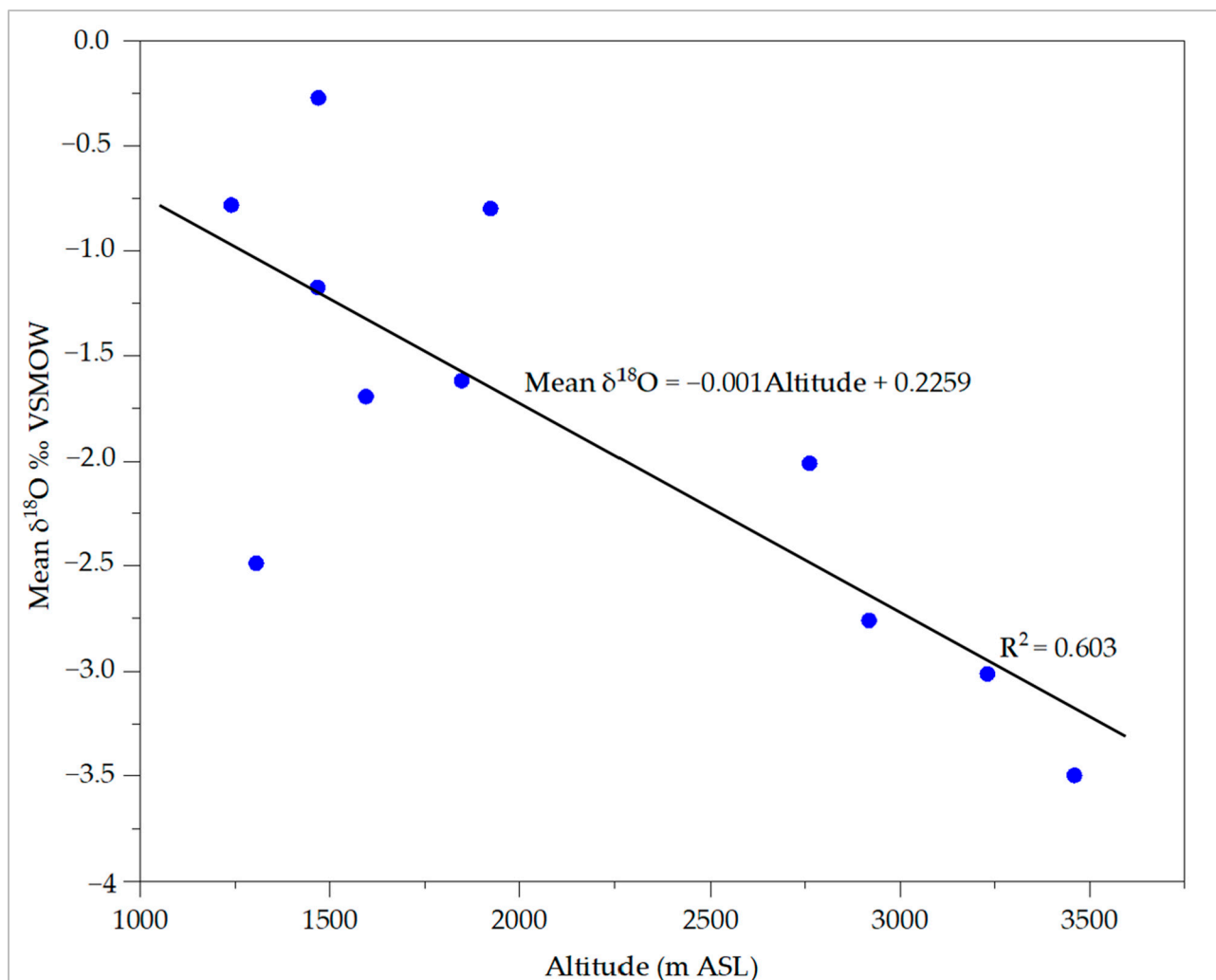


Figure 10. Altitude effect on heavy isotope ($\delta^{18}\text{O}$) values in regional precipitation.

To determine if there is a significant difference in D-excess between the two rainy seasons (MAM and SON) (Figures S4 and S5), a statistical *t*-test was conducted (Figure S9). This test was appropriate for assessing whether a statistical difference existed between the D-excess values for these two seasons. The paired *t*-test results showed a *t*-statistic of 1.929 and a *p*-value of 0.066. Since the *p*-value is greater than the common significance level of 0.05, there is no evidence to reject the null hypothesis [70]. Therefore, there is no statistically significant difference in D-excess between the MAM and SON rains at the 5% significance level.

3.6. Analysis of Stable Isotope in Groundwater

Eighteen groundwater samples (seventeen from Cluster B and one from Cluster A) plot along and close to the D-parameter line that also plots above the Global Meteoric Waterline (Figure 11). One groundwater sample (in Cluster A) plots below the Global Meteoric Waterline. Cluster A consists of groundwater samples that are more enriched in heavy isotopes relative to Cluster B samples. This can be attributed to evaporative enrichment imposed on Cluster A samples prior to groundwater recharge possibly from

depression storage and slow groundwater recharge as a consequence of the prevalence of impervious formations such as shales and phyllites that are dominant in the study area (Figure 1).

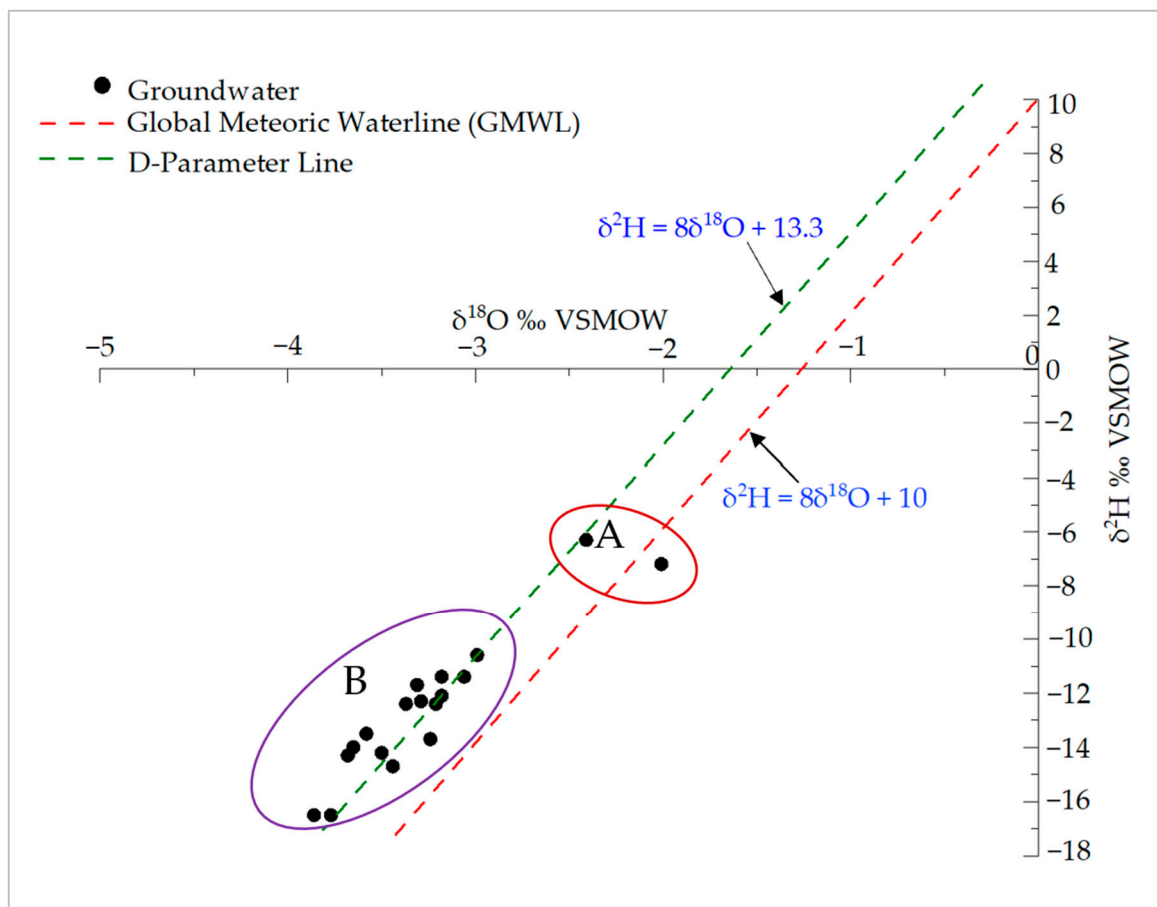


Figure 11. Distribution of groundwater samples along the D-parameter line and GMWL.

One groundwater sample in Cluster A plots away from the D-parameter line (Figure 11). This groundwater sample (RAF7021-25) was collected at Masha within the granite gneiss at lower hydraulic elevations (Figure 2). The isotopic shift of this sample can be attributed to high-temperature chemical reactions relative to its sister groundwater sample in the same cluster. The graphical model in (Figure 11) clearly indicates that groundwater in the project area originates from local precipitation. This is evidenced by 90% of the groundwater samples plotting along and close to the D-parameter line. This signifies that both groundwater and local precipitation share a common moisture source [52].

3.7. Tritium Isotope Analysis

Tritium results reveal clusters of groundwater samples based on their respective relative ages (Figure 12). Ten groundwater samples (marked in red) clustered in the lower eastern and northwestern regions have tritium units below the detection limit of 0.4, indicating groundwater likely older than 20 years. These samples cover areas of Masha, Kaberebere, Isingiro, Kakamba, Rugaga and Mbaare. Conversely, nine samples (marked in green) have tritium units above 0.4, indicating recently recharged groundwater (likely less than 20 years old). This dating approach was adopted due to the lack of historical tritium measurements in precipitation for the region and the study area, in particular, from the Global Network of Isotopes in Precipitation (GNIP) website.

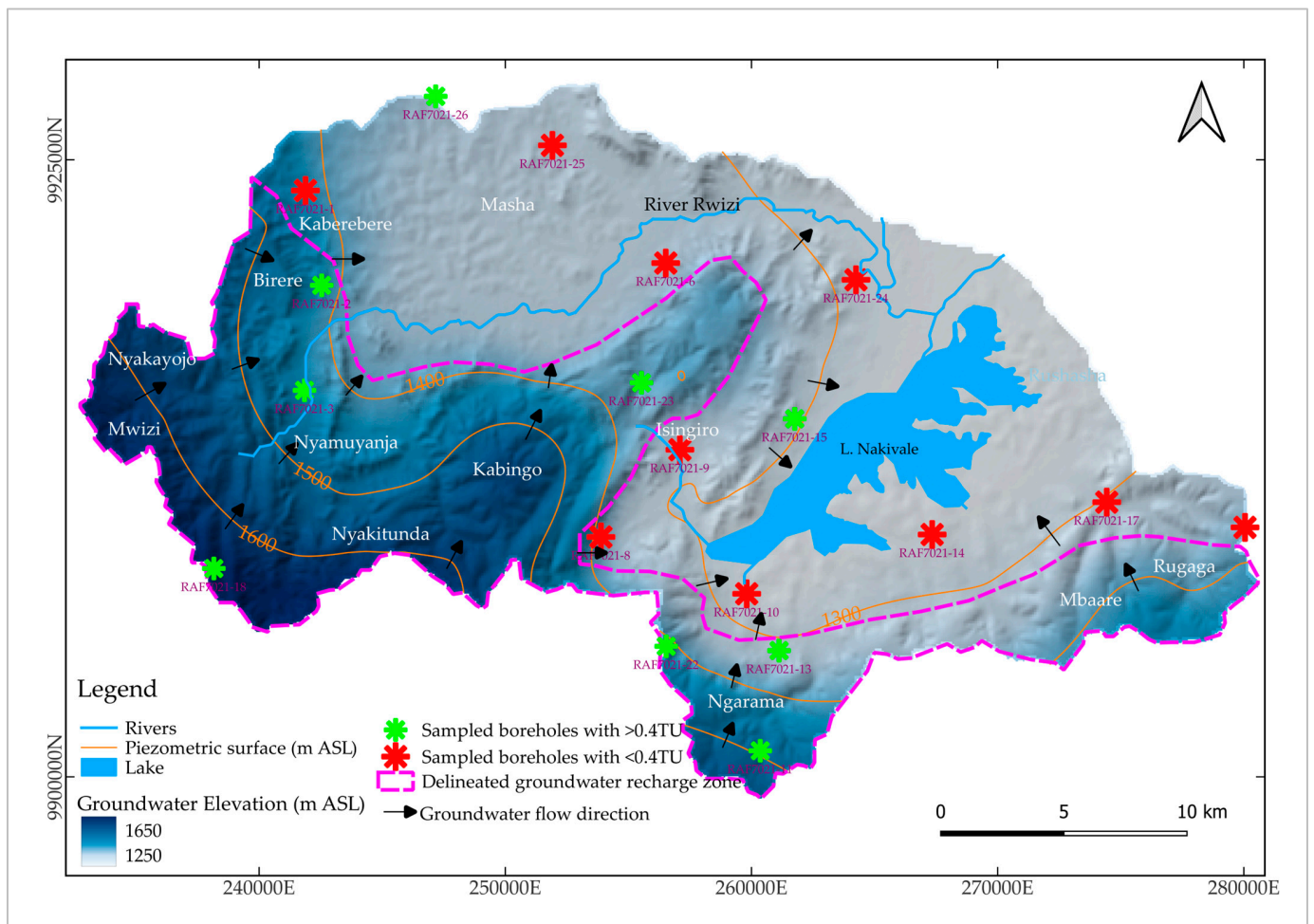


Figure 12. Clustering of groundwater samples based on their relative ages and delineated groundwater recharge zones within the Nakivale sub-catchment.

The tritium analysis results align with those of [32], which identified old groundwater in the region characterized by very low tritium values (<0.4 TU). This groundwater is believed to reside within pockets of paleochannels formed by historic river reversals due to the down-warping and uplifting of the Ugandan plateau [34]. Additionally, the results align with findings from the Chebotarev sequence (Figure 5), which suggest the aging of groundwater toward the Masha and Nakivale areas. These findings point to slow groundwater recharge and movement within the underlying aquifer systems, underscoring the need for careful management of this invaluable resource.

3.8. Groundwater Recharge Assessment

Groundwater recharge zones correlate to topographically high areas characterized by a network of lineament features which facilitate groundwater infiltration into the underlying aquifers. Groundwater generally flows from these elevated regions with high hydraulic gradients to discharge areas situated within lowlands of the study area (see Figure 13). Additionally, these zones exhibit low Cl/Br ratios (Figure S13). According to [71], areas with a low Cl/Br ratio may signify active groundwater recharge zones. The low Cl/Br ratio in areas close to Lake Nakivale may be attributed to preferential organic adsorption of chloride [72]. This pattern is further supported by high tritium values (>0.4 TU), highlighting active recharge in elevated areas, in contrast to the lower tritium values (<0.4 TU) observed in the low-lying regions of Masha and Lake Nakivale.

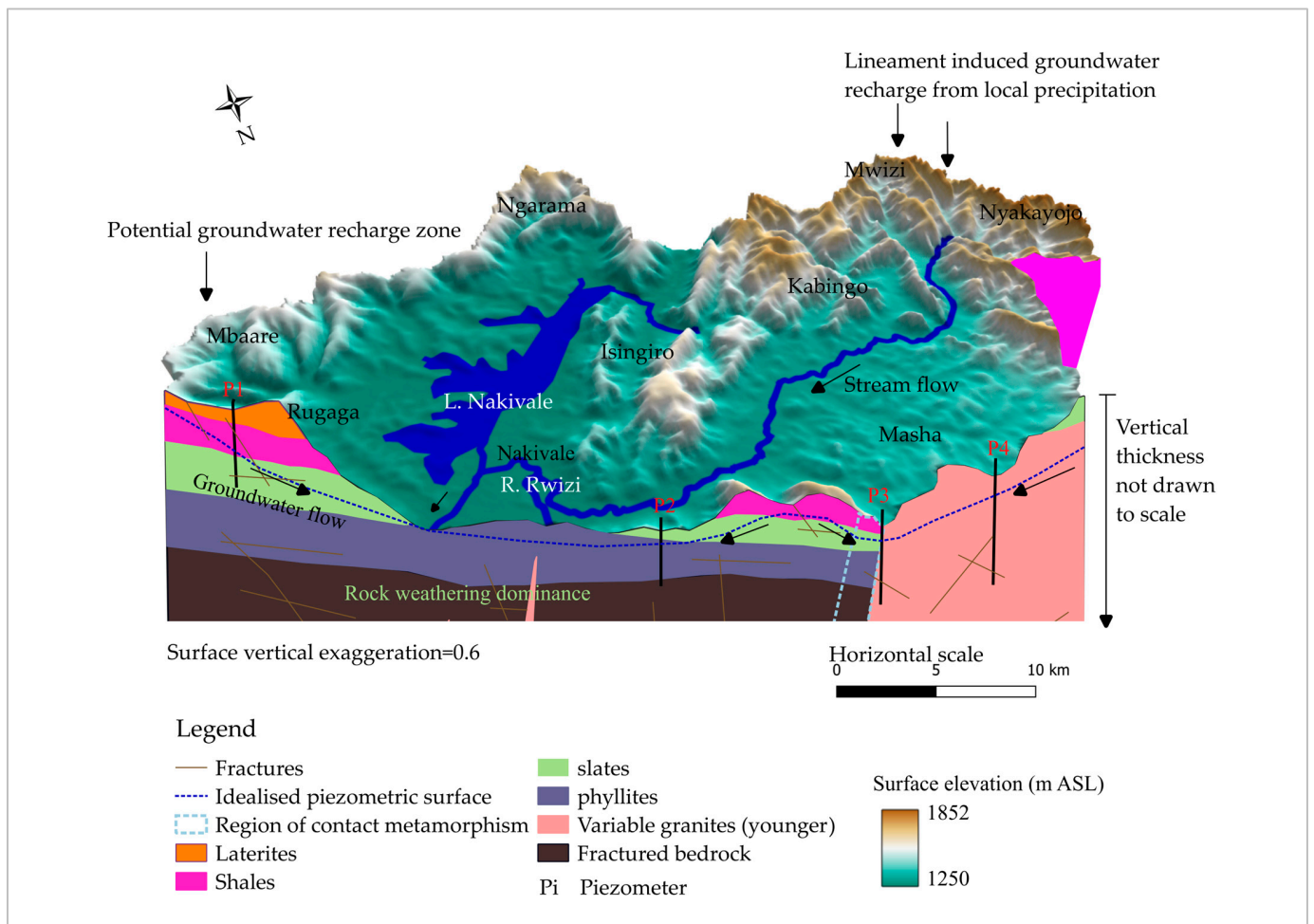


Figure 13. Conceptual site model showing major groundwater recharge areas, hydro-stratigraphy, and geological structures in the Nakivale sub-catchment.

4. Conclusions and Recommendations

4.1. Conclusions

This study has comprehensively examined groundwater resources within the Nakivale sub-catchment in Isingiro district, southwestern Uganda using both classical hydrochemistry and isotopic approaches.

The predominant groundwater type in the study area is Ca-SO_4 . The cationic facies are ordered by relative abundance as $\text{Ca} > \text{Mg} > \text{Na} > \text{K}$, while the anionic species are ordered as $\text{SO}_4 > \text{HCO}_3 > \text{Cl}$. Groundwater hydrochemistry is primarily influenced by water–rock interaction processes, including the weathering of plagioclase and alkali feldspars, as well as mafic minerals. Calcium is mainly derived from the weathering of Ca-rich plagioclase feldspars and sulphate primarily from the oxidation of sulfide minerals like pyrite which are predominant in the study area. Key weathering processes identified include dissolution, hydrolysis, hydration, and carbonation.

Groundwater recharge and flow in the study area is primarily influenced by the topographical makeup evidenced by a high hydraulic head and low chloride–bromide ratio in elevated areas. The elevated areas have dense lineament networks that facilitate groundwater infiltration into underlying aquifers. These recharge areas include Birere, Nyakayonjo, Mwizi, Nyamuyanja, Kabingo, Rugaga, and the southern parts of Rugaga. The findings are underscored by the evidence of the Chebotarev sequence along groundwater flow lines (Figure 5). This sequence involves the transitioning of groundwater-dominant anionic facies from bicarbonate to chloride dominance. This pattern is consistent with the spatial

recharge–discharge gradient, where bicarbonate-rich water is prevalent in topographically high areas, while chloride-rich water characterizes lowland discharge zones.

Isotopic analysis reveals that the groundwater primarily originates from local precipitation. Tritium data indicate the presence of both recent and older groundwater, with some samples from Masha, Kaberebere, and Kakamba suggesting groundwater age likely older than 20 years. The tritium analysis results are consistent with the findings of [32], who identified old groundwater water in the region characterized by very low tritium values (less than 0.4 TU).

4.2. Implications to Water Resources Management

The Ministry of Water and Environment plays a crucial role in ensuring the sustainable management of groundwater resources in Uganda. Groundwater is vital for agricultural, domestic, and industrial uses, significantly contributing to the region's economic growth and development. With low groundwater recharge rates (50–100 mm/year) and the presence of old water in the region (evidenced by low tritium levels < 0.4 TU), coupled with projected rising water demand (7.85 MCM/year) by 2040, it is essential to balance groundwater availability and demand for both current and future generations. As Uganda aims for upper middle-income status by 2040, immediate action is needed to protect this invaluable resource from depletion conditions. This study provides critical insights into the current state of groundwater, highlighting key challenges and opportunities for enhanced management. The following recommendations are proposed to ensure the long-term sustainability of groundwater in the region:

- A robust groundwater monitoring network should be established to continuously assess both water quality and quantity in the study area. Regular hydrochemical and isotopic analyses will allow for tracking changes over time and identifying emerging contamination sources. This approach has been successfully implemented in California, where extensive groundwater monitoring programs support effective water management [73].
- To protect identified recharge areas from contamination and over-extraction, it is crucial to enforce land-use regulations and promote conservation practices. Controlling agricultural runoff, preventing industrial discharges, and encouraging reforestation in critical zones will help safeguard these areas. The Guangzhou Greenway Initiative in China serves as an example of how stringent land-use regulations can protect and enhance groundwater recharge areas [74].
- Community awareness programs should be developed to educate local populations on groundwater conservation and sustainable usage practices. Involving communities in monitoring activities fosters ownership and responsibility, which leads to better water management. The “Waterkeeper” movement in the USA and Canada has demonstrated how community engagement can significantly improve water quality and conservation efforts [75].
- An integrated approach to water resource management is necessary, considering the interdependencies between surface and groundwater. A rigorous IWRM framework should address the needs of all water users while ensuring sustainable use. The Murray–Darling Basin Plan in Australia showcases how integrated management across states can promote long-term water sustainability [76].
- Investing in infrastructure such as check dams, infiltration ponds, and wastewater treatment facilities is essential, particularly in urban and industrialized areas where contamination risks are higher. The state of Gujarat in India provides a successful example, where the construction of check dams and recharge wells has significantly improved groundwater levels and quality [77].

4.3. Limitations of the Study and Directions for Future Research

While this study provides valuable insights into the hydrochemical and isotopic characteristics of groundwater in the Nakivale sub-catchment, it also acknowledges the following limitations and potential areas for future research:

- The study focused on a relatively small region (the Nakivale sub-catchment) and sampled only a limited number of groundwater points. A larger-scale study could offer a more comprehensive view of regional groundwater dynamics increasing the relevance and applicability of the findings to other parts of southwestern Uganda and potentially the broader Great Lakes region. Future research should consider expanding the study area to include additional catchments, which could help determine whether the observed hydrochemical and isotopic patterns are consistent across the region.
- The study largely relied on data collected at a specific point in time, potentially missing seasonal or long-term variations in groundwater quality, recharge patterns, or isotopic signatures. Future studies should incorporate temporal data by conducting long-term monitoring of groundwater quality and isotopic compositions across different seasons and years to assess temporal variability and the impacts of climate change.
- The study's reliance on tritium data from groundwater samples without historical tritium measurements from local precipitation presents a limitation. The lack of precipitation tritium data in the region introduces uncertainties in groundwater age dating. To improve the accuracy of groundwater age assessments, future studies should aim to include tritium analysis for local precipitation and establish a more reliable baseline for interpreting tritium in groundwater.
- The hydrochemical processes in the study area are influenced by various geological formations, including shales, phyllites, and granite gneiss. However, the study may not have fully accounted for all local geological heterogeneities, such as fault zones, fractures, and mineral variations, which could influence groundwater chemistry in specific locations. Future research could involve detailed geological mapping and hydrogeological modelling to better understand how different geological formations influence groundwater flow and chemistry in the region.

Supplementary Materials: The following supporting information can be downloaded at: <https://www.mdpi.com/article/10.3390/w16233394/s1>, Figure S1: Mineral saturation index vs. electrical conductivity; Figure S2: Piper diagram showing the groundwater types within the study area; Figure S3: Partial pressure of carbon dioxide vs. pH bivariate plot; Figure S4: D-excess variation in precipitation received within the study area for MAM rainy season (data source: GNIP website); Figure S5: D-excess variation in precipitation received within the study area for SON rainy season (data source: GNIP website); Figure S6: Soil type map for Nakivale sub-catchment; Figure S7: Histogram showing D-excess values for local precipitation received within Nakivale sub-catchment; Figure S8: A box plot showing descriptive statistics of D-excess for local precipitation received in Nakivale sub-catchment; Figure S9: Paired student's t-test results for MAM and SON D-excess values for rainfall received within Nakivale sub-catchment; Figure S10: Hydrochemical analysis laboratory certificate; Figure S11: Stable isotope analysis laboratory certificate; Figure S12: Tritium analysis laboratory certificate; Figure S13: Spatial distribution of chloride–bromide ratio across Nakivale sub-catchment; Table S1: Summary of the used precipitation data obtained from 11 isotope stations on the Global Network of Isotopes in Precipitation (GNIP) website; Table S2: Charge balance error (CBE) computation for the analyzed hydrochemical samples; Table S3: Correlation matrix for analyzed hydrochemical species; Table S4: Stable isotopes in precipitation data for Masaka Station in Uganda; Table S5: Groundwater types for each sample: classified based on dominant ions in meq/L.

Author Contributions: Conceptualization, E.N.H. and R.M.K.; methodology, E.N.H. and R.M.K.; software, E.N.H.; validation, E.N.H. and R.M.K.; formal analysis, E.N.H. and R.M.K.; investigation, E.N.H.; resources, E.N.H. and R.M.K.; data curation, E.N.H. and R.M.K.; writing—original draft preparation, E.N.H.; writing—review and editing, E.N.H., R.M.K., and C.M.; visualization, E.N.H.; supervision, R.M.K.; project administration, E.N.H.; funding acquisition, E.N.H., R.M.K., and C.M. All authors have read and agreed to the published version of the manuscript.

Funding: This research was funded by the International Atomic Energy Agency (IAEA) under the RAF7021 project, in partnership with the Ministry of Water and Environment of Uganda. The research was conducted during a fellowship (code: EVT2304936-0001-UGA) hosted by the University of Strathclyde, United Kingdom, from 9 October 2023 to 8 November 2024.

Data Availability Statement: All the data used in this research have been provided within the attached Supporting Information.

Acknowledgments: The authors gratefully acknowledge IAEA TC Project RAF7021 for the invaluable financial support extended throughout all stages of the project's implementation. The authors are also thankful for the financial support of the Scottish Government under the Climate Justice Fund Water Futures Program (research grant HN-CJF-03), awarded to the University of Strathclyde (R.M. Kalin PI).

Conflicts of Interest: The authors declare no conflicts of interest.

References

1. Ministry of Water and Environment. *National Water Resources Assessment Report*; Ministry of Water and Environment: Kampala, Uganda, 2013.
2. African Union. *Agenda 2063 Framework Document*; African Union: Addis Ababa, Ethiopia, 2015.
3. United Nations Environment Programme. Goal 6: Clean Water and Sanitation. 2024. Available online: <https://www.unep.org/explore-topics/sustainable-development-goals/why-do-sustainable-development-goals-matter/goal-6> (accessed on 10 November 2024).
4. National Planning Authority. *The National Development Plan 4 Strategic Direction*; Ministry of Finance, Planning and Economic Development: Kampala, Uganda, 2024.
5. World Bank. *Uganda Vision. 2040: A Transformed Ugandan Society from a Peasant to a Modern and Prosperous Country Within 30 years*. 2013. Available online: <https://consultations.worldbank.org/content/dam/sites/consultations/doc/migration/vision20204011.pdf> (accessed on 9 November 2024).
6. Ministry of Water and Environment. *Rwizi Catchment Management Plan*; Ministry of Water and Environment: Kampala, Uganda, 2020.
7. Ministry of Water and Environment. *National Groundwater Resources Availability and Demand. Assessment for Uganda*; Ministry of Water and Environment: Kampala, Uganda, 2023; *to be submitted*.
8. Ministry of Water and Environment. *National Water Resources Assessment of Uganda*; Ministry of Water and Environment: Kampala, Uganda, 2011.
9. Ministry of Water and Environment. *Baseline Groundwater Assessment Report-National Groundwater Study*; Ministry of Water and Environment: Kampala, Uganda, 2023; *to be submitted*.
10. Owor, M.; Taylor, R.; Mukwaya, C.; Tindimugaya, C. Groundwater/surface-water interactions on deeply weathered surfaces of low relief: Evidence from Lakes Victoria and Kyoga, Uganda. *Hydrogeol. J.* **2011**, *19*, 1403. [[CrossRef](#)]
11. Asmael, N.M.; Huneau, F.; Garel, E.; Celle-Jeanton, H.; Le Coustumer, P.; Dupuy, A.; Hamid, S. Origin and recharge mechanisms of groundwater in the upper part of the Awaj River (Syria) based on hydrochemistry and environmental isotope techniques. *Arab. J. Geosci.* **2015**, *8*, 10521–10542. [[CrossRef](#)]
12. Banda, L.C.; Kalin, R.M.; Phoenix, V. Isotope hydrology and hydrogeochemical signatures in the Lake Malawi Basin: A multi-tracer approach for groundwater resource conceptualisation. *Water* **2024**, *16*, 1587. [[CrossRef](#)]
13. Belkhiri, L.; Tiri, A.; Mouni, L. Spatial distribution of the groundwater quality using kriging and Co-kriging interpolations. *Groundw. Sustain. Dev.* **2020**, *11*, 100473. [[CrossRef](#)]
14. Fraser, C.M.; Kalin, R.M.; Rivett, M.O.; Nkhata, M.; Kanjaye, M. A national approach to systematic transboundary aquifer assessment and conceptualisation at relevant scales: A Malawi case study. *J. Hydrol. Reg. Stud.* **2018**, *20*, 35–48. [[CrossRef](#)]
15. Kalin, R.M.; Long, A. *Application of Hydrogeochemical Modelling for Validation of Hydrologic Flow Modelling in the Tucson Basin Aquifer, Arizona, United States of America*; U.S. Department of Energy Office of Scientific and Technical Information: Oak Ridge, TN, USA, 1994.
16. Owor, M.; Muwanga, A.; Tindimugaya, C.; Taylor, R.G. Hydrogeochemical processes in groundwater in Uganda: A national-scale analysis. *J. Afr. Earth Sci.* **2021**, *175*, 104113. [[CrossRef](#)]
17. Pradhan, R.M.; Behera, A.K.; Kumar, S.; Kumar, P.; Biswal, T.K. Recharge and geochemical evolution of groundwater in fractured basement aquifers (NW India): Insights from environmental isotopes ($\delta^{18}\text{O}$, $\delta^2\text{H}$, and 3H) and hydrogeochemical studies. *Water* **2022**, *14*, 315. [[CrossRef](#)]
18. Shuaibu, A.; Kalin, R.M.; Phoenix, V.; Banda, L.C.; Lawal, I.M. Hydrogeochemistry and water quality index for groundwater sustainability in the Komadugu-Yobe Basin, Sahel Region. *Water* **2024**, *16*, 601. [[CrossRef](#)]
19. Uganda Bureau of Statistics. *Census Population Counts (2002 and 2014) by Region, District, and Mid-Year Population Projections (2015–2021)*. 2023. Available online: <https://www.ubos.org/explore-statistics/20/> (accessed on 7 September 2024).

20. Bjørkhaug, I. Revisiting the refugee host relationship in Nakivale Refugee Settlement: A dialogue with the Oxford Refugee Studies Centre. *J. Migr. Hum. Secur.* **2020**, *8*, 266–281. [[CrossRef](#)]
21. Fletcher, R.D. The general circulation of the tropical and equatorial atmosphere. *J. Atmos. Sci.* **1945**, *2*, 167–174. [[CrossRef](#)]
22. Nagudi, B.; Status of Geological Resources in Uganda. For the Embassy of the Republic of Korea in Uganda. 2011. Available online: https://www.korcham.net/new_doc/Biz_Down/%EC%9A%B0%EA%B0%84%EB%8B%A4%EA%B4%91%EB%AC%BC%EC%9E%90%EC%9B%90%ED%98%84%ED%99%A9%EB%B3%B4%EA%B3%A0%EC%84%9C.pdf (accessed on 7 September 2024).
23. Doornkamp, J.C. The role of inselbergs in the geomorphology of southern Uganda. *Trans. Inst. Br. Geogr.* **1968**, 151–162. [[CrossRef](#)]
24. Stheeman, H.A.; Stheeman, H.A. Various Phases of Folding-Nature of Contact-Manner of Intrusion. *Geol. Southwest. Uganda Spec. Ref. Stanniferous Depos.* **1932**, 53–64.
25. Combe, A.; Holmes, A. The kalsilite bearing lavas of Kabirenge and Lyakauli. South West Uganda. *Trans. R. Soc. Edinb.* **1945**, *62*, 359–379. [[CrossRef](#)]
26. Pohl, W. Metallogeny of the northeastern Kibara belt, Central Africa-Recent perspectives. *Ore Geol. Rev.* **1994**, *9*, 105–130. [[CrossRef](#)]
27. Singhal, B.B.S.; Gupta, R.P.; Singhal, B.B.S.; Gupta, R.P. Hydrogeology of crystalline rocks. *Appl. Hydrogeol. Fract. Rocks* **1999**, 241–260.
28. Shirazi, S.M.; Adham, M.I.; Zardari, N.H.; Ismail, Z.; Imran, H.M.; Mangrio, M.A. Groundwater quality and hydrogeological characteristics of Malacca state in Malaysia. *J. Water Land. Dev.* **2015**, 11–19. [[CrossRef](#)]
29. Cook, P.G. *A Guide to Regional Groundwater Flow in Fractured Rock Aquifers*; CSIRO: Canberra, Australia, 2003.
30. Taylor, R.G.; Howard, K.W.F. Post-Palaeozoic evolution of weathered landsurfaces in Uganda by tectonically controlled deep weathering and stripping. *Geomorphology* **1998**, *25*, 173–192. [[CrossRef](#)]
31. Tindimugaya, C. *Groundwater Flow and Storage in Weathered Crystalline Rock Aquifer Systems of Uganda*; University of London, University College London: London, UK, 2007.
32. Tindimugaya, C.; Gaye, C.B. *Use of Isotopes in the Management of Kisoro Town Water Supply, Uganda*; Directorate of Water Development, Ministry of Water, Lands and Environment, Entebbe: Kampala, Uganda, 2003.
33. Leeder, M.R.; Leeder, M.R. Grain properties. In *Sedimentology: Process and Product*; Chapman and Hall: London, UK, 1982; pp. 35–43.
34. Williams, M. *The Nile Basin: Quaternary Geology, Geomorphology and Prehistoric Environments*; Cambridge University Press: Cambridge, UK, 2019.
35. Anderson, W.; Glauber, J.; Mamun, A.; You, L.; Thurlow, J.; Jamali, A. Presentations for Implications of El Niño 2023/24 for Africa South of the Sahara. 2024. Available online: https://scholar.google.com/scholar?hl=en&as_sdt=0,5&q=Presentations+for+Implications+of+El+Ni%C3%B1o+2023/24+for+Africa+South+of+the+Sahara&btnG= (accessed on 8 October 2024).
36. Singh, M.; Ouedraogo, M.; Kagabo, D. El Niño 2023–2024 status and its possible impact on food security in African continent. 2023. Available online: <https://cgspace.cgiar.org/server/api/core/bitstreams/73a9c93c-2f4b-43f8-b555-94e63e196c30/content> (accessed on 8 October 2024).
37. Maliva, R.G.; Coulibaly, K.; Guo, W.; Missimer, T.M. Confined aquifer loading: Implications for groundwater management. *Groundwater* **2011**, *49*, 302–304. [[CrossRef](#)]
38. Broekaert, J.A.C. *Inductively Coupled Plasma Spectrometry. Handbook of Spectroscopy: Second Enlarged Edition*; Wiley: Hoboken, NJ, USA, 2014.
39. Hou, X. Liquid scintillation counting for determination of radionuclides in environmental and nuclear application. *J. Radioanal. Nucl. Chem.* **2018**, *318*, 1597–1628. [[CrossRef](#)]
40. Piper, A.M. A graphic procedure in the geochemical interpretation of water-analyses. *Eos Trans. Am. Geophys. Union* **1944**, *25*, 914–928.
41. Gibbs, R.J. Mechanisms controlling world water chemistry. *Science* **1970**, *170*, 1088–1090. [[CrossRef](#)] [[PubMed](#)]
42. Fentahun, A.; Mechal, A.; Karuppappan, S. Hydrochemistry and quality appraisal of groundwater in Birr River Catchment, Central Blue Nile River Basin, using multivariate techniques and water quality indices. *Env. Environ. Monit. Assess.* **2023**, *195*, 655. [[CrossRef](#)] [[PubMed](#)]
43. Belkhir, L.; Boudoukha, A.; Mouni, L. A multivariate statistical analysis of groundwater chemistry data. *Int. J. Environ. Res.* **2011**, *5*, 537–544.
44. Lawley, D.N.; Maxwell, A.E. Factor analysis as a statistical method. *J. R. Stat. Soc. Ser. D* **1962**, *12*, 209–229. [[CrossRef](#)]
45. Koul, V.K.; Davison, W.; Zutshi, D.P. Calcite supersaturation in some subtropical, Kashmir, Himalayan lakes. *Hydrobiologia* **1990**, *192*, 215–222. [[CrossRef](#)]
46. Larson, T.E.; Buswell, A.M.; Ludwig, H.F.; Langelier, W.F. Calcium carbonate saturation index and alkalinity interpretations. *J. Am. Water Works Assoc.* **1942**, *34*, 1667–1684. [[CrossRef](#)]
47. Myers, D.E. Kriging hydrochemical data. In *Current Trends in Geomathematics*; Springer: Boston, MA, USA, 1988; pp. 117–142.
48. Oliver, M.A.; Webster, R. Kriging: A method of interpolation for geographical information systems. *Int. J. Geogr. Inf. Syst.* **1990**, *4*, 313–332. [[CrossRef](#)]
49. Aladejana, J.A.; Kalin, R.M.; Hassan, I.; Sentenac, P.; Tijani, M.N. Origin and residence time of groundwater in the shallow coastal aquifer of eastern Dahomey basin, southwestern Nigeria, using $\delta^{18}\text{O}$ and δD isotopes. *Appl. Sci.* **2020**, *10*, 7980. [[CrossRef](#)]

50. Craig, H. Isotopic variations in meteoric waters. *Science* **1961**, *133*, 1702–1703. [[CrossRef](#)]
51. McDonnell, J.J.; Kendall, C. *Isotope Tracers in Hydrology*; John Wiley and Sons: Hoboken, NJ, USA, 1992.
52. Kendall, C.; Caldwell, E.A. Fundamentals of isotope geochemistry. In *Isotope Tracers in Catchment Hydrology*; Elsevier: Amsterdam, The Netherlands, 1998; pp. 51–86.
53. Lindsey, B.D.; Jurgens, B.C.; Belitz, K. *Tritium as an Indicator of Modern, Mixed, and Premodern Groundwater Age (No. 2019–5090)*. US Geological Survey; USGS: Reston, VA, USA, 2019.
54. Schlosser, P.; Stute, M.; Dörr, H.; Sonntag, C.; Münnich, K.O. Tritium/³He dating of shallow Groundwater. *Earth Planet Sci. Lett.* **1988**, *89*, 353–362. [[CrossRef](#)]
55. Marandi, A.; Shand, P. Groundwater chemistry and the Gibbs Diagram. *Appl. Geochemistry*. **2018**, *97*, 209–212. [[CrossRef](#)]
56. Chebotarev, I.I. Metamorphism of natural waters in the crust of weathering-1. *Geochim. Cosmochim. Acta* **1955**, *8*, 22–48. [[CrossRef](#)]
57. Hilberg, S.; Brandstätter, J.; Glück, D. CO₂ partial pressure and calcite saturation in springs—useful data for identifying infiltration areas in mountainous environments. *Env. Environ. Sci. Process Impacts* **2013**, *15*, 823–832. [[CrossRef](#)] [[PubMed](#)]
58. Mandalaparty, P.; Deo, M.; Moore, J. Gas-compositional effects on mineralogical reactions in carbon dioxide sequestration. *SPE J.* **2011**, *16*, 949–958. [[CrossRef](#)]
59. Chorley, R.J. The role of water in rock disintegration. In *Introduction to Fluvial Processes*; Routledge: Milton Park, UK, 2019; pp. 53–73.
60. Zhang, D.; Xue, T.; Xiao, J.; Chai, N.; Gong, S.G. Significant influence of water diversion and anthropogenic input on riverine sulfate based on sulfur and oxygen isotopes. *J. Hazard. Mater.* **2024**, *461*, 132622. [[CrossRef](#)]
61. Kocabağ, D. The Oleophilicity/Hydrophobicity of Galena and Pyrite in Two-Liquid Flotation. Ph. D. Thesis, University of London, London, UK, 1983.
62. Fuge, R. Sources of halogens in the environment, influences on human and animal health. *Env. Environ. Geochem. Health* **1988**, *10*, 51–61. [[CrossRef](#)]
63. Moloantoa, K.M.; Khetsha, Z.P.; Van Heerden, E.; Castillo, J.C.; Cason, E.D. Nitrate water contamination from industrial activities and complete denitrification as a remediation option. *Water* **2022**, *14*, 799. [[CrossRef](#)]
64. Abascal, E.; Gómez-Coma, L.; Ortiz, I.; Ortiz, A. Global diagnosis of nitrate pollution in groundwater and review of removal technologies. *Sci. Total Environ.* **2022**, *810*, 152233. [[CrossRef](#)]
65. Farmer, V.C. Sources and speciation of aluminium and silicon in natural waters. In *Ciba Foundation Symposium 121-Silicon Biochemistry: Silicon Biochemistry: Ciba Foundation Symposium 121*; John Wiley & Sons: Chichester, UK, 2007; pp. 4–23.
66. Akpataku, K.V.; Rai, S.P.; Gnazou, M.D.T.; Tampo, L.; Bawa, L.M.; Djaneye-Boundjou, G.; Faye, S. Hydrochemical and isotopic characterization of groundwater in the southeastern part of the Plateaux Region, Togo. *Hydrol. Sci. J.* **2019**, *64*, 983–1000. [[CrossRef](#)]
67. Coplen, T. Stable Isotope Hydrology: Deuterium and Oxygen-18 in the Water Cycle. *EOS Trans. Am. Geophys. Union* **1982**, *63*, 861–862. [[CrossRef](#)]
68. Anyah, R.O.; Semazzi, F.H.; Xie, L. Simulated physical mechanisms associated with climate variability over Lake Victoria basin in East Africa. *Mon. Weather. Rev.* **2006**, *134*, 3588–3609. [[CrossRef](#)]
69. Beverly, E.J.; White, J.D.; Peppe, D.J.; Faith, J.T.; Blegen, N.; Tryon, C.A. Rapid Pleistocene desiccation and the future of Africa’s Lake Victoria. *Earth Planet. Sci. Lett.* **2020**, *530*, 115883. [[CrossRef](#)]
70. Goodman, S.N.; Royall, R. Evidence and scientific research. *Am. J. Public. Health* **1988**, *78*, 1568–1574. [[CrossRef](#)] [[PubMed](#)]
71. Goldowitz, J. *The Chloride to Bromide Ratio as an Environmental Groundwater Tracer, with a Field Study at the Wellton-Mohawk Irrigation and Drainage District*; The University of Arizona: Tucson, AZ, USA, 1989.
72. Nailly, W. Cl/Br ratio to determine groundwater quality. *IOP Conf. Ser. Earth Environ. Sci.* **2018**, *118*, 012020. [[CrossRef](#)]
73. Calderwood, A.J.; Pauloo, R.A.; Yoder, A.M.; Fogg, G.E. FGE Low-cost, open source wireless sensor network for real-time, scalable groundwater monitoring. *Water* **2020**, *12*, 1066. [[CrossRef](#)]
74. Chen, S.; Wang, Y.; Ni, Z.; Zhang, X.; Xia, B. Benefits of the ecosystem services provided by urban green infrastructures: Differences between perception and measurements. *Urban. For. Urban. Green.* **2020**, *54*, 126774. [[CrossRef](#)]
75. Martin, M.; Webb, K. Water quality protection of the Canada-US Great Lakes: Examining the emerging state/nonstate governance approach. *Int. J. Innov. Sustain. Dev.* **2020**, *14*, 102–124. [[CrossRef](#)]
76. Hart, B.T. The Australian Murray–Darling Basin plan: Challenges in its implementation (part 1). *Int. J. Water Resour. Dev.* **2016**, *32*, 819–834. [[CrossRef](#)]
77. Chinnasamy, P.; Misra, G.; Shah, T.; Maheshwari, B.; Prathapar, S. Evaluating the effectiveness of water infrastructures for increasing groundwater recharge and agricultural production—A case study of Gujarat, India. *Agric. Water Manag.* **2015**, *158*, 179–188. [[CrossRef](#)]

Disclaimer/Publisher’s Note: The statements, opinions and data contained in all publications are solely those of the individual author(s) and contributor(s) and not of MDPI and/or the editor(s). MDPI and/or the editor(s) disclaim responsibility for any injury to people or property resulting from any ideas, methods, instructions or products referred to in the content.